Mon. Not. R. astr. Soc. (1981) **197**, 107–138

Nova Cygni 1978 – I. The nebular phase

D. J. Stickland *Royal Greenwich Observatory, Herstmonceux Castle, Hailsham, E. Sussex BN27 1RP*

C. J. Penn, M. J. Seaton, M. A. J. Snijders and P. J. Storey *Department of Physics and Astronomy, University College London, Gower Street, London WC1E 6BT*

Received 1981 January 16; in original form 1980 October 10

Summary. UV observations of Nova Cygni 1978, which were obtained using *IUE* on 17 dates between 1978 September 12 and 1979 July 8 inclusive, will be discussed in the present series of papers. Paper I is mainly concerned with the interpretation, during the nebular stage, of the UV observations together with optical and IR data from other observers.

The adopted value of the reddening, $E(B-V) = 0.4 \pm 0.1$ from the 2200 Å feature, is in satisfactory agreement with values deduced by other methods. The total observed flux, F(obs), is obtained from UV, optical and IR observations as a function of D, the number of days after outburst. The maximum value, F(max), of F(obs) occurs on $D = 6$ and between $D = 13$ and $D = 27$, F(obs) has an approximately constant value of $0.30F$(max); subsequently F(obs) declines. The estimated Eddington luminosity of the remnant is $L(\mathrm{E}) = 5 \times 10^4 L_\odot$. The luminosity L(max) obtained from F(max) is equal to L(E) for a distance of $d = 2.2$ kpc. This value is adopted; it is in good agreement with the value obtained by Duerbeck *et al.* from the relation between reddening and distance in the direction to the nova, but less than the value of $d = 3.6$ kpc deduced from the relation between decay time and maximum absolute visual magnitude.

The UV spectra show emission lines of: He II; C II, III and IV; N II, III, IV and V; O I, II, III, IV and V; and Mg II. The lines C II λ 1335, C III λ 2297 and N IV λ 1718 are produced by dielectronic recombination via low-lying autoionizing states. Electron temperatures are deduced from the flux ratios (C II λ 1335)/(C III] λ 1908), (C III λ 2297)/(C IV λ 1549) and (N IV λ 1718)/(N V λ 1240). Ion abundances relative to He^{2+} are obtained for three ionization stages of C, four of N, and four of O.

Abundances relative to H^+ are obtained using optical data of Klare *et al.* and *IUE* observations of the H I Balmer continuum. Element abundances relative to H, by number, are 0.12 for He, 0.008 for C, 0.021 for N and 0.017

for O. They are enhanced, relative to the Sun, by factors of 20 for total CNO and 200 for N, indicating that the nova was produced by a thermonuclear runaway.

The best observations for the UV continuum, obtained on $D = 70$, are interpreted as due to recombination and free–free emission of ions of H, He, C, N and O and radiation from a stellar remnant with a temperature of 1.5×10^5 K and a radius of $0.13 R_\odot$.

There is reasonable agreement between values of the ionized ejected mass, M_i, estimated using electron densities deduced from forbidden lines and estimated using measured expansion velocities. The value adopted is $M_i = 1.1 \times 10^{29}$ g and the corresponding kinetic energy is 6×10^{44} erg. The ionized mass may be equal to the total ejected mass, but this is not certain.

The onset of thermal infrared emission is probably due to pre-existing dust heated by absorption of radiation in UV resonance lines.

1 Introduction

We discuss the interpretation of observations of Nova Cygni 1978, both those which we have obtained in the ultraviolet using the *IUE* satellite and those obtained by other workers at optical and infrared wavelengths. Our study indicates that Nova Cygni 1978 was produced by a mechanism involving a thermonuclear runaway.

1.1 THE THERMONUCLEAR RUNAWAY MECHANISM

The production of novae by mechanisms involving thermonuclear runaways is discussed by Starrfield, Truran & Sparks (1978), who give references to earlier work; further references are given in a review by Gallagher & Starrfield (1978). It is supposed that hydrogen-rich material is accreted on to a white dwarf in a binary system. At the base of the hydrogen envelope the density becomes sufficiently large for the equation of state to be that of a degenerate electron gas and the temperature rises to a value at which hydrogen can burn in the CNO cycle. Since the degenerate gas pressure is insensitive to temperature, a thermonuclear runaway occurs and is halted only when the temperature rises to a value sufficiently large to lift the degeneracy. During the runaway the main nuclear reactions are proton captures, such as $^{12}C(p,\gamma)^{13}N$ and $^{13}N(p,\gamma)^{14}O$. Some of the nuclei produced subsequently undergo β^+ decays, such as $^{13}N(\beta^+\nu)^{13}C$ and $^{14}O(\beta^+\nu)^{14}N$ but the decay lifetimes are larger than the time duration of the runaway event. The rate of energy production during the runaway is determined by the initial abundances of the CNO elements and detailed computations show that this rate will be sufficient to produce ejection of a shell only if the CNO abundances are substantially larger than abundances in the Sun. If this mechanism is operative, the computations show that: (i) the ejected material will have enhanced CNO abundances; (ii) the abundance of N will be enhanced, relative to C and O; (iii) for some time after ejection of the shell the remnant continues to have a high luminosity, due to hydrostatic hydrogen burning.

It is of interest to establish whether these predictions are confirmed by observations. Early evidence for enhanced CNO abundances in nova shells was obtained by Mustel & Boyarchuk (1959) and by Pottasch (1959). More recent confirmation has come from optical observations of the shell surrounding DQ Her (Williams *et al.* 1978) and of the nebular stage of V1500 Cyg, Nova Cygni 1975 (Ferland & Shields 1978). Evidence that the luminosity remains large for some time after outburst was obtained by Gallagher & Code (1974) who,

using *OAO–A2*, obtained UV observations of FH Ser. These showed that during the first 60 days after outburst the decline in visual magnitude was due to an increase of the temperature and hence to a shift of radiation into the UV.

Important new advances should come from UV observations with higher spectral resolution which can be obtained with *IUE*.

1.2 NOVA CYGNI 1978

Nova Cygni 1978 (V1668 Cyg) was a moderately fast classical nova. We give day numbers D relative to the date of outburst, taken to be 1978 September 7.5, following Gehrz *et al.* (1980). Photometric observations are reported by Duerbeck, Rindermann & Seitter (1980) for *UBV*, Gallagher *et al.* (1980) for *uvby*, Joseph, Kessler & Selby (1981) for *JHKLM* and Gehrz *et al.* (1980) for 14 bands from V to [19.5 μm]. Visual maximum occurred on $D \simeq 4$ with $m_v = 6.2$ and the time for decay by 3 mag was $t_3 = 30$ days. The infrared emission rose steeply from $D \simeq 35$ and had a maximum on $D \simeq 60$.

A pre-maximum optical spectrum was obtained by Fehrenbach & Andrillat (1979) and optical spectra were obtained by Klare, Wolf & Krautter (1980) during the period $D = 4$–102. These showed the nebular stage to be reached by $D = 59$.

Nova Cygni 1978 was probably the first nova to be observed with *IUE*. Observations were obtained by teams from each of the three participating agencies, NASA (Wu *et al.* 1979), ESA (Cassatella *et al.* 1979) and SRC (Stickland *et al.* 1979).

1.3 THE SRC OBSERVATIONS USING *IUE*

Our observations were obtained from *IUE*, under control of the VILSPA tracking station, in connection with an SRC scheme for observations of 'targets of opportunity'. Table 1 gives details of dates, image numbers (LWR for longwave, SWP for shortwave), aperture (S for small, L for large), exposure duration and mean day numbers D. Notes give further information, particularly on regions of saturation. The present paper is mainly concerned with the interpretation of results obtained during the nebular stage. Other aspects of the interpretation of the UV observations will be published later.

1.4 THE NEBULAR EMISSION LINES

The emission lines from the nebular shell are produced by two mechanisms, recombination and electron impact excitation.

For a recombination line of an ion A^{m+} the emissivity is proportional to

$$N(A^{(m+1)+})N_e \tag{1.1}$$

multiplied by a slowly varying function of electron temperature T_e; $N(A^{n+})$ is the number density of ions A^{n+} and N_e is the electron density.

For lines excited by electron impacts we first consider the case for which collisional de-excitation can be neglected. For a line of an ion A^{m+} excited by electron impacts the emissivity is then proportional to

$$N(A^{m+})N_e \exp(-\Delta E/kT_e), \tag{1.2}$$

where ΔE is the excitation energy. The collisionally excited lines observed in the UV are mostly permitted lines and intercombination lines. At earlier dates the density may be

Table 1. *IUE* observations of Nova Cygni 1978 obtained under the target of opportunity programme of the UK SRC.

Date*	Image number	Aperture	Exposure duration (min)	Notes	Mean day number
1978 Sep.11.69	LWR 2323	S	1	1	
11.70		L	5	3	4.2
11.72	SWP 2627	S	1	2	
11.73		L	3	1	
12.72	SWP 2636	L	25	1	
12.74		S	5	2	
12.75	LWR 2335	S	15	4	5.2
12.78		L	3	5	
15.71	SWP 2655	L	35	6	
15.74	LWR 2365	L	18	7	8.2
15.76		S	3	8	
19.73	LWR 2407	S	2	9	
19.74		L	10	10	
19.75	SWP 2697	S	30	11	12.3
19.78		L	2	1	
23.96	LWR 2448	L	8	12	
23.97		S	2	13	
23.97	SWP 2742	S	20	14	16.5
23.99		L	3	1	
Oct. 15.89	SWP 2990	S	10	15	
15.90		L	1	1	38.4
17.77	LWR 2633	L	4	16	
17.77		S	1	1	
17.78	SWP 3011	L	5	17	40.3
17.78		S	3	1	
25.65	LWR 2709	S	15	18	48.1
25.69	LWR 2710	S	100	19	48.2
29.85	SWP 3190	S	3	1	
29.85		L	6	20	
29.88	LWR 2751	S	1.5	2	52.4
29.88		L	6	21	
Nov. 6.59	LWR 2841	L	6	22	
6.60		S	2	23	
6.62	SWP 3237	L	240	24	60.2
6.81	SWP 3238	L	9	25	
6.82		S	3	1	
16.58	LWR 2946	S	4	1	
16.58		L	8	26	
16.59	SWP 3362	S	4	27	
16.60		L	9	28	70.1
16.62	LWR 2947	L	90	29	
16.81	LWR 2948	L	25	30	
Dec. 4.65	SWP 3526	S	3	1	
4.66		L	9	31	
4.67	LWR 3100	S	5	1	88.2
4.68		L	12	32	
26.66	LWR 3285	L	15	33	
26.68		S	5	1	
26.68	SWP 3714	S	3	1	110.2
26.69		L	12	34	
1979 Jan.13.46	SWP 3908	S	3.5	2	
13.46		L	40	34	
13.50	LWR 3478	S	6	1	128.0
13.51		L	45	35	

Table 1 – *continued*

Date*	Image number	Aperture	Exposure duration (min)	Notes	Mean day number
March 6.19	SWP 4505	S	60	36	
6.24		L	10	1	179.7
6.25	LWR 3942	S	30	1	
6.28		L	8	23	
24.25	LWR 4100	L	32	1	
24.28	SWP 4737	L	25	1	197.8
24.31	LWR 4101	L	96	1	
July 8.93	SWP 5755	L	300	37	304.4

* Exposure starting time in UT.

Notes: Exposures are low resolution unless otherwise stated; regions of saturation are preceded by S. (1) Good spectrum. (2) Very underexposed. (3) S: 2500–end. (4) S: 2617–2771, 2794–end. (5) S: 2814–2819, 2884–3052, 3071–3095. (6) S: 1794–1799, 1866–1888, 1936–end. (7) S: 2408–end. (8) S: 2631–2640, 2794–2836, 2874–3037. (9) S: 2626–2636, 2794–2818, 2893–2916, 2949–2959, 2981–3019. (10) S: 2412–3268. (11) S: 1788–1806, 1862–1884, 1935–end. (12) S: 2408–3221. (13) S: 2636–2645, 2766–2827, 2902–2916, 2949–2958, 2967–3014. (14) S: 1744–end. (15) S: 1301–1309. (16) S: 2632–2641, 2964–2973, 2992–2997. (17) S: 1300–1305, 1746–1748. (18) High resolution, underexposed. (19) High resolution, slightly underexposed. (20) S: 1305–1310. (21) S: 2324–2338, 2735–2782, 2791–2824, 2838–2880. (22) S: Mg II λ 2800. (23) Underexposed. (24) High resolution, S: 1744–1746, C III] λ 1909. (25) S: O I λ 1303, C II λ 1335, N III] λ 1750, C III] λ 1909. (26) S: Mg II λ 2800. (27) S: C III] λ 1909. (28) S: C IV λ 1550, N III] λ 1750, C III] λ 1909. (29) High resolution, good spectrum. (30) S: C III] λ 1909, C II] λ 2326, 2506–2529, 2730–2955. (31) S: N IV] λ 1486, C IV λ 1550, N III] λ 1750, C III] λ 1909. (32) S: C III] λ 1909, C II] λ 2326, Mg II λ 2800. (33) S: C III] λ 1909, C II] λ 2326, Mg II λ 2800. (34) S: N V 1240, N IV] λ 1486, C IV λ 1550, N III] λ 1750, C III] λ 1909. (35) S: C III] λ 1909. C II] λ 2326, Mg II λ 2800. (36) S: C III] λ 1909. (37) S: C IV λ 1550, C III] λ 1909.

sufficiently high for there to be significant collisional de-excitation of the intercombination lines. In the present paper we consider later dates, for which such effects can be neglected.

The collisionally excited lines observed in the optical spectra of nova shells are forbidden lines with small radiative transition probabilities A_{21}. In many cases the density is such that collisional de-excitation cannot be neglected for these lines. If the collisional de-excitation probability, $q_{21}N_e$, is large compared with A_{21} the levels have Boltzmann distributions and the emissivity is proportional to

$$N(A^{m+})\,A_{21}\exp(-\Delta E/kT_e). \tag{1.3}$$

A difficulty which arises in attempting to deduce abundances from optical spectra of nova shells is that the ratios of fluxes in recombination lines and forbidden lines may depend on N_e. A further difficulty is that ion abundances can be obtained for only a small number of ionization stages. Much more complete information on ion abundances can be deduced from UV observations.

1.5 ELECTRON TEMPERATURES

The expressions (1.2) and (1.3) are sensitive to T_e, particularly for the UV lines. The key to the interpretation of the observed line fluxes therefore lies in the determination of electron temperatures.

In a preliminary report (Stickland *et al.* 1979) we used the intensity ratios

$$\frac{(\text{C II } 2s2p^2\ ^2D \rightarrow 2s^2 2p\ ^2P^0\ \lambda 1335)}{(\text{C II } 2s\ 2p^2\ ^4P \rightarrow 2s^2 2p\ ^2P^0\ \lambda 2326)} \tag{1.4}$$

and

$$\frac{(\text{C III } 2p^2\ ^1D \rightarrow 2s\ 2p\ ^1P^0\ \lambda 2297)}{(\text{C III } 2s\ 2p\ ^3P^0 \rightarrow 2s^2\ ^1S\ \lambda 1909)} \tag{1.5}$$

to determine T_e, assuming all of the lines involved to be excited by electron impacts. This gave values of T_e in the range 2×10^4–5×10^4 K. Subsequent work has shown that these temperatures are too large. Important clues are provided by observations of C II λ 1335 and C III λ 2297 in the spectra of planetary nebulae (Clavel, Flower & Seaton 1981; Harrington, Lutz & Seaton 1979) for which the electron temperatures are known to be too low for the lines to be excited by electron impacts. A further clue is provided by the C^+/C^{2+} ionization equilibrium deduced from *IUE* observations of the planetary nebula IC 418 (Harrington *et al.* 1980); the observed ratio was unexpectedly large and Harrington *et al.* suggested that it might be explained by dielectronic recombination of C^{2+} to C^+ via low-lying auto-ionizing states. Further studies have now been made and it is found that dielectronic recombination can explain the observed ionization equilibrium and can also provide an efficient mechanism for production of the lines C II λ 1335, C III λ 2297 and N IV λ 1718. This work will be described briefly in Section 5.1 and in more detail elsewhere (Storey 1981). Since low-lying auto-ionizing states are involved, the effective recombination rates are insensitive to electron temperature. This mechanism gives the following ratios to be sensitive to T_e

(C II λ1335)/(C III] λ 1909),

(C III λ 2297)/(C IV λ 1549), (1.6)

(N IV λ 1718)/(N V λ 1240).

It is these ratios which are used in the present paper to determine electron temperatures.

2 Observations

2.1 THE UV NEBULAR LINES

The UV spectra of Nova Cygni 1978 contain strong lines and many weak lines. Since the *IUE* cameras have a rather low dynamic range, the strong lines are saturated in spectra for which the weak lines are well exposed. For most dates on which we made *IUE* observations we therefore obtained two spectra for each of the two *IUE* cameras (long wave and short wave) using the large and the small apertures, with exposure times chosen to give good flux measurements for both strong lines and weaker lines. The transmission of the small aperture was determined from features well observed in both apertures. The data were reduced using a correct intensity transfer function.

Fig. 1 shows composite spectra for $D = 88$. Table 2 gives results for the nebular lines discussed in the present paper. The columns give: line identifications; notes; and observed line fluxes $F_0(\lambda)$ for day numbers $D = 70$, 88, 110, 128, 180, 198 and 304. The accuracy of the fluxes for the strong lines is generally about 10 per cent, corresponding to the accuracy of *IUE* photometric calibration. Measurements which are less accurate are marked with a colon and for these comments on accuracy are given in the notes. The notes also give references to atomic rate coefficients used in the present work.

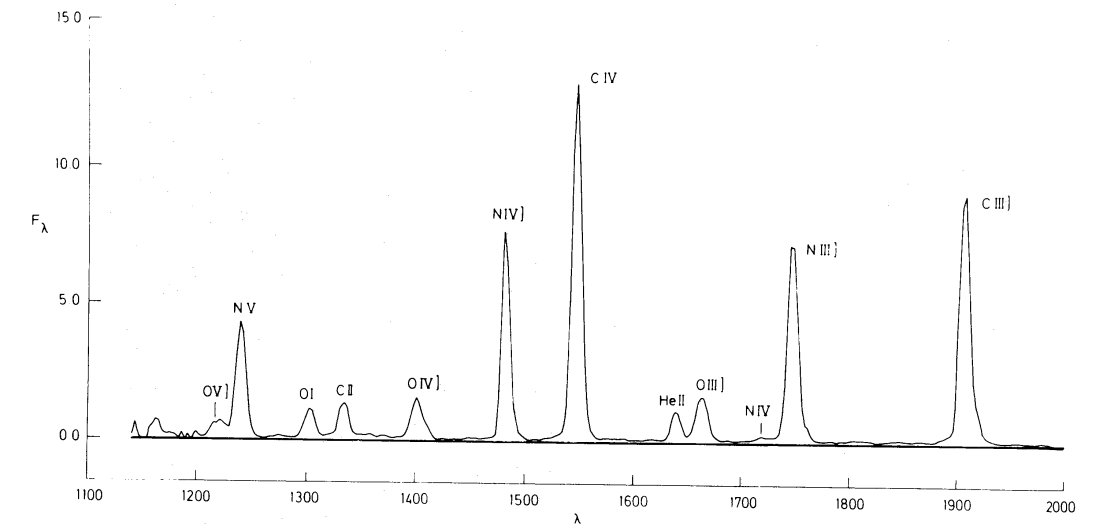

(a)

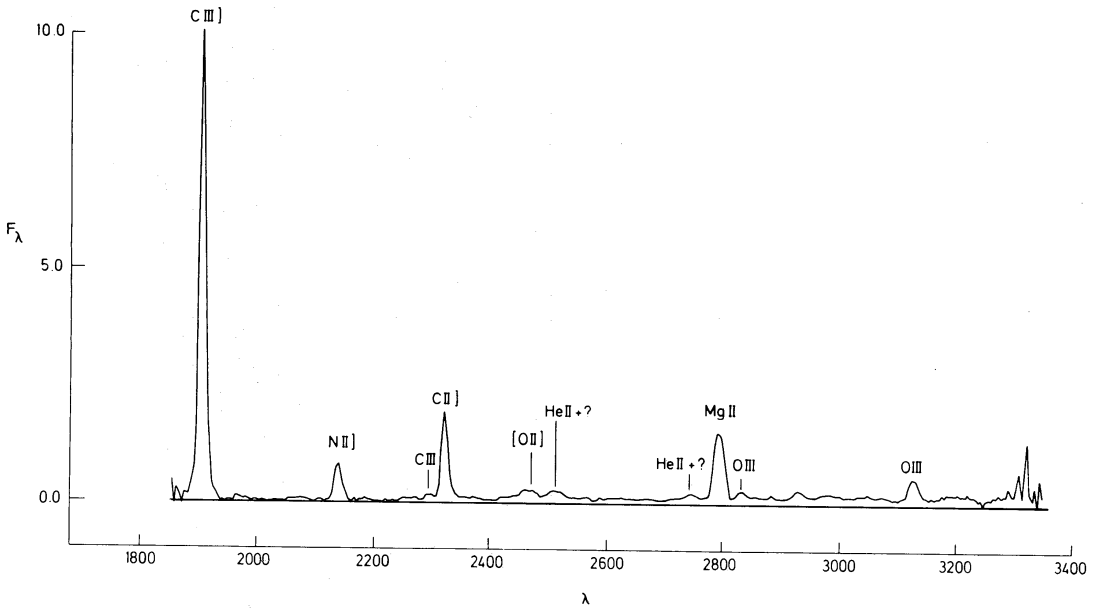

(b)

Figure 1. Composite *IUE* spectra of Nova Cygni 1978 for $D = 88$ (1978 December 4) Fluxes in units 10^{-12} erg cm^{-2} s^{-1} Å^{-1}. (a) Short wave spectra from SWP 3526, small and large aperture. (b) Long wave spectra from LWR 3100, small and large aperture.

Caution is required in measuring fluxes for weak lines. Errors may arise due to blending with unidentified features. The magnitude of such errors may be estimated by considering two pairs of lines for which the relative fluxes should be known. The first pair is O III λ 3133 and λ 2837. These lines are produced by the Bowen mechanism, to be discussed in Section 10.1, and the expected ratio of fluxes is $F(2837)/F(3133) = 0.10$. The line at λ 3133 is fairly strong and the measured flux should be reliable. There is a feature at $\lambda \simeq 2837$ but the measured flux is too strong, by a factor of at least 2, for the feature to be due entirely to O III λ 2837. The second pair is He II λ 1640 and λ 3202, for which the ratio of fluxes is given by recombination theory. The calculated ratio of observed fluxes, corrected for extinction (see Section 3.1), is $F_0(1640)/F_0(3202) = 6$. The observed ratio is 11 for $D = 88$, 10 for $D = 110$ and 3 for $D = 198$. We conclude that the measured flux for the weak line,

Table 2. List of transitions, wavelengths, measured fluxes*, notes on atomic data (numerical notes) and notes on data quality (alphabetical notes).

Atom/ion	λ (Å)	Transition	Notes	log 10^{15} F (erg cm^{-2} s^{-1})†						
				D = 70	88	110	128	180	198	304
He II	1640	$3 \rightarrow 2$	1	4.27	4.03	3.80	3.50	2.97	2.74	2.33
He II	3202	$5 \rightarrow 3$	a	–	2.97:	2.81:	–	–	2.32:	–
C II	1335	$2s\,2p^2\,{}^2D \rightarrow 2s^2\,2p\,{}^2P^0$	3 h	4.50	4.17	4.01	3.75	3.09:	3.09	2.55
C II]	2326	$2s\,2p^2\,{}^4P \rightarrow 2s^2\,2p\,{}^2P^0$	2	4.53	4.45	4.28	4.16	3.32	3.18	–
C III]	1909	$2s\,2p\,{}^3P^0 \rightarrow 2s^2\,{}^1S$	4 k	5.16:	5.06	4.87:	4.57	3.86	3.64	2.88:
C III	2297	$2p^2\,{}^1D \rightarrow 2s\,2p\,{}^1P^0$	3 c	3.40:	3.41:	2.81:	2.65:	2.23:	2.14:	–
C IV	1549	$2p\,{}^2P^0 \rightarrow 2s\,{}^2S$	5 l	4.93	5.14	5.03	4.67	4.03	3.83	3.18:
N II]	2140	$2s\,2p^3\,{}^5S^0 \rightarrow 2s^2\,2p^2\,{}^3P$	2	4.15	4.09	3.82	3.55	2.85	2.34	–
[N II]	3063	$2s^2\,2p^2\,{}^1S \rightarrow 2s^2\,2p^2\,{}^3P$	6	–	3.04	3.03	–	–	–	–
N III]	1750	$2s\,2p^2\,{}^4P \rightarrow 2s^2\,2p\,{}^2P^0$	2	5.02	4.94	4.76	4.44	3.71	3.48	2.78
N IV]	1486	$2s\,2p\,{}^3P^0 \rightarrow 2s^2\,{}^1S$	7	4.71	4.84	4.73	4.31	3.77	3.63	2.99
N IV	1718	$2p^2\,{}^1D \rightarrow 2s\,2p\,{}^1P^0$	3 d	3.45:	3.16:	3.23:	3.01:	2.10:	2.31:	1.75:
N V	1240	$2p\,{}^2P^0 \rightarrow 2s\,{}^2S$	8	4.31	4.51	4.62	4.30	3.70	3.48	2.75
O I	1303	$2p^3\,3s\,{}^3S^0 \rightarrow 2p^4\,{}^3P$	9 e	4.48	4.07	3.62	3.25:	2.12:	1.01:	0.90:
O I]	1356	$2p^3\,3s\,{}^5S^0 \rightarrow 2p^4\,{}^3P$	f	3.64:	3.13	2.76	2.42	2.10:	1.88:	0.77:
[O II]	2470	$2s^2\,2p^3\,{}^2P^0 \rightarrow 2s^2\,2p^3\,{}^4S^0$	10 b	3.44:	3.42:	3.32:	3.03:	2.74:	2.51:	–
O III]	1663	$2s\,2p^3\,{}^5S^0 \rightarrow 2s^2\,2p^2\,{}^3P$	11 i	4.39	4.33	4.20	3.91	3.20:	2.94	2.28
O III	3133	$2p\,3d\,{}^3P^0 \rightarrow 2p\,3p\,{}^3S$	13 m	3.92:	3.93:	3.79:	3.57:	2.75:	2.94:	–
O IV]	1402	$2s\,2p^2\,{}^4P \rightarrow 2s^2\,2p\,{}^2P^0$	12 j	4.17	4.29	4.19	3.96	3.35	3.01	2.54
O V]	1218	$2s\,2p\,{}^3P^0 \rightarrow 2s^2\,{}^1S$	4	–	3.68	3.83	–	3.09	–	–
O V	1370	$2p^2\,{}^1D \rightarrow 2s\,2p\,{}^1P^0$	3 g	2.88:	2.98:	2.73:	2.50:	1.67:	2.10:	1.59:

* Fluxes are uncorrected for interstellar reddening.

† Errors on line intensities are less than 10 per cent unless indicated by a colon.

Notes: References to sources of atomic data (1) Brocklehurst (1971). (2) Jackson (1973). (3) Storey (1981). (4) Dufton *et al.* (1978). (5) Taylor *et al.* (1977). (6) Seaton (1975). (7) Collision strengths interpolated from calculations for C III and O V. (8) Wyngaarden & Henry (1976). (9) Excited by Lyβ fluorescence. (10) Pradhan (1976). (11) Baluja, Kingston & Burke (1980). (12) Collision strength of Hayes – private communication. (13) Saraph & Seaton (1980).

Percentage errors due to estimation of continuum level and other comments (a) ± 70 per cent for D = 88, 198; ± 60 per cent for D = 110. (b) ± 35 per cent for D = 88, 110; ± 50 per cent for D = 70; errors of a factor 2 for D = 128–198; (blended with an unidentified line of approximately the same strength). (c) ± 20 per cent for D = 70, 88, 198; ± 40 per cent for D = 110; ± 60 per cent for D = 128, 180. (d) ± 40 per cent for D = 70, 88; ± 20 per cent for D = 110, 198, 304; ± 50 per cent for D = 128, 180. (e) ± 15 per cent for D = 128; errors of a factor 2 for D = 180, 304. (f) ± 20 per cent for D = 70; ± 70 per cent for D = 88; ± 40 per cent for D = 110; ± 90 per cent for D = 128, 198; values given are upper limits only for D = 180, 304. (g) ± 30 per cent for D = 70, 304; ± 80 per cent for D = 88, 128; ± 45 per cent for D = 110; ± 65 per cent for D = 198; a factor 2 for D = 180. (h) ± 13 per cent for D = 180. (i) ± 14 per cent for D = 180. (j) Blended with Si IV; Si IV contribution < 10 per cent. (k) Lower limit to flux for D = 70, 110, 304. (l) Lower limit to flux for D = 304. (m) ± 17 per cent for D = 70, 110; ± 20 per cent for D = 88, 198; ± 13 per cent for D = 128; ± 38 per cent for D = 180.

λ 3202, can be in error by factors of about 2. Similar errors may occur in measurements for other weak lines, such as N IV λ 1718, which are of importance for the work of the present paper.

Several identifications have been considered and rejected. A feature at $\lambda \simeq 2423$ is considered not to be due to [Ne IV] λ 2423. The Ne IV multiplet has a very low radiative transition probability and if the Ne abundance were sufficiently high for it to be observed, we would expect to observe a number of other neon forbidden lines, such as [Ne III] λ 1814, [Ne IV] λ 1602 and [Ne V] λ 1575 and λ 2975. We can set upper limits to the fluxes in these lines which lead us to reject the [Ne IV] λ 2423 identification. Another rejected identification is [Mg V] λ 2929. A second member of the same multiplet is at λ = 2784 and the calculated flux ratio is $F(2784)/F(2929) = 3.6$. There is an observed feature at λ = 2929 but no detectable feature at λ = 2784.

2.2 THE UV CONTINUUM AND UNRESOLVED WEAK LINES

The UV spectra in the nebular stage show, in addition to the stronger lines, a background due to continuum emission and unresolved very weak lines. Our best observations for this background were obtained on $D = 70$, for which we obtained three LWR exposures and two SWP exposures. For each wavelength we obtain a composite flux by adding fluxes from unsaturated exposures, weighted by exposure times. The 25-min exposure LWR 2948 (large slot), which is saturated in most of the stronger lines, is valuable in giving our best determination of the flux in the region of 2200 Å and also at the longest wavelengths observable with *IUE*.

The lower part of Fig. 2 shows our composite spectrum for $D = 70$. We here use a log–log plot and truncate the strong emission lines. There is seen to be clear evidence for the interstellar absorption feature centred at 2200 Å.

2.3 THE OPTICAL OBSERVATIONS

Plots of relative fluxes I_λ in the optical spectra of Nova Cygni 1978 are given by Klare *et al.* (1981). The *IUE* observations give absolute fluxes $F(\lambda)$ in erg cm^{-2} s^{-1}. We may put $F(\lambda) = K(\lambda) I_\lambda$ where $K(\lambda)$ varies slowly with λ and is the same for all dates on which optical observations were made (Klare 1980, private communication). We estimate $K(\lambda)$ for λ = 4686 and 5755 Å. For the former we use the ratio of fluxes in the He II lines λ 1640 and λ 4686 and assume case B recombination theory (Seaton 1978; for case B it is assumed that the emitting region is optically thick for Lyman lines and optically thin for all other lines). For λ 5755 we use the ratio of fluxes in the [N II] lines λ 3063 and λ 5755, which have a common upper state, $N^+ 2p^2\,{}^1S$, and a known branching ratio.

3 Reddening, distance and expansion velocity

3.1 REDDENING

Let $F_0(\lambda)$ be an observed flux, $F(\lambda)$ the corresponding flux corrected for extinction. Then

$$F(\lambda) = F_0(\lambda)\, 10^{0.4 E(B-V) X_\lambda}, \tag{3.1}$$

where for the function X_λ we use the analytical fit to observations adopted by Seaton (1979). The upper curve on Fig. 2 shows the flux for $D = 70$ corrected for extinction using

$$E(B-V) = 0.4. \tag{3.2}$$

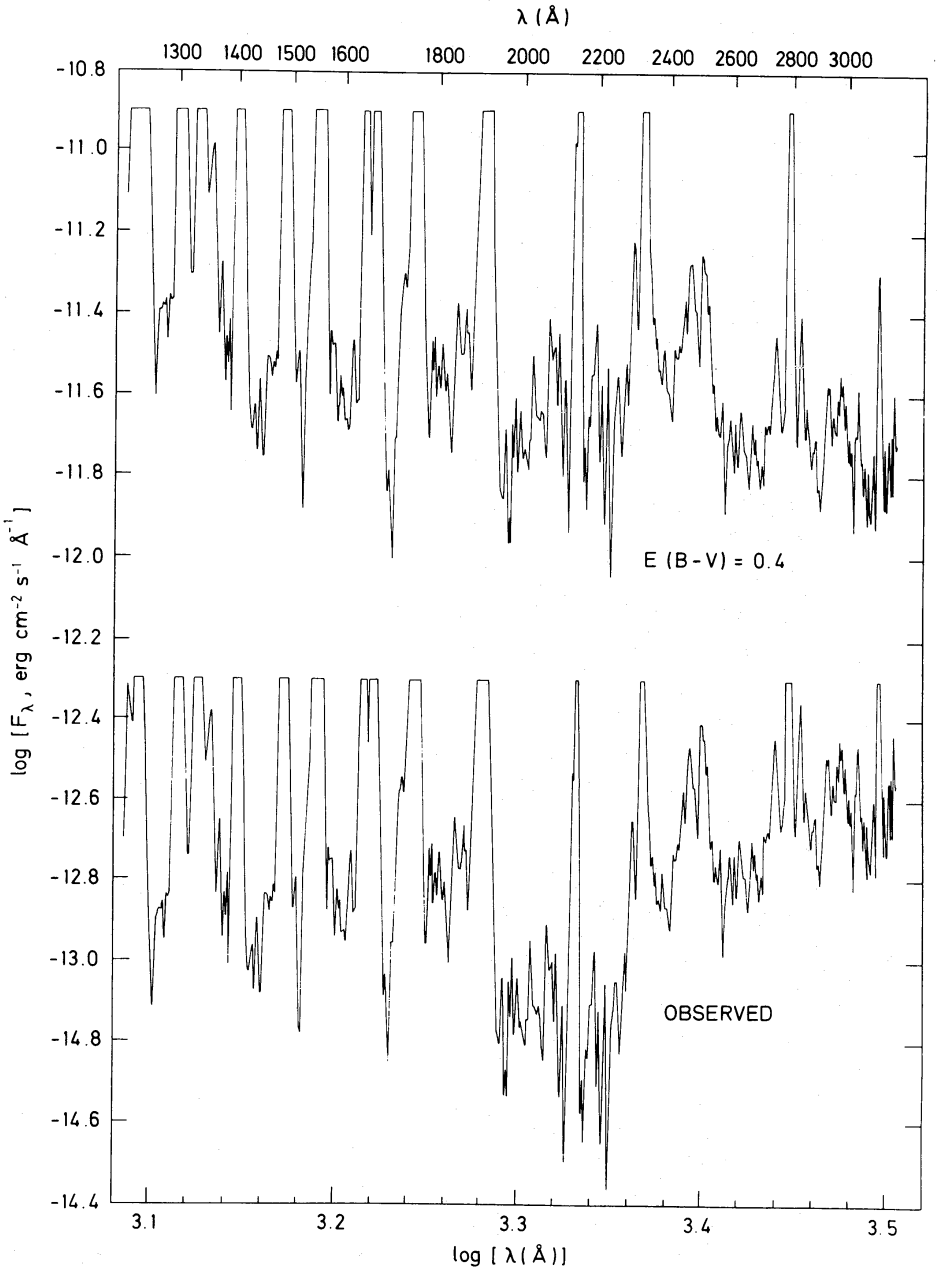

Figure 2. Composite spectra of Nova Cygni 1978 for D = 70 (1978 November 16), plotted on logarithmic scales to show the continuum and weak lines. The strong lines are truncated. The lower curve shows the observed flux, the upper curve shows the flux corrected for extinction using $E(B-V) = 0.4$.

It is seen that this gives no discernible feature at 2200 Å. A feature is discernible for $E(B-V) \geqslant 0.5$ or $E(B-V) \leqslant 0.3$. We conclude that $E(B-V) = 0.4 \pm 0.1$. This is consistent with $E(B-V) = 0.35 \pm 0.08$ adopted by Duerbeck *et al.* (1980) as a mean of values deduced from various observations at optical wavelengths. We adopt $E(B-V) = 0.4$ in all subsequent work.

3.2 DISTANCE

The relation

$$M_v = -11.5 + 2.5 \log t_3 \qquad (3.3)$$

between the absolute visual magnitude at maximum and the time in days for the visual magnitude to decline by three magnitudes is given by Schmidt (1957) and McLaughlin (1960). Canterna & Schwartz (1977) discuss the use of equation (3.3) for Nova LMC 1977b, which has a value of t_3 similar to that of Nova Cygni 1978. Using equation (3.3) they obtain a distance for Nova LMC 1977b which is in good agreement with the best estimates for the distance of the LMC determined by other methods (see Crampton 1979).

For Nova Cygni 1978 we have, as noted in Section 1, $m_v = 6.2$ at maximum and $t_3 = 30$ days. With $E(B-V) = 0.4$ we have $A_V = 1.2$ and (3.3) gives a distance of $d = 3.6$ kpc. This value is in agreement with $d = 3.3 \pm 0.6$ kpc obtained by Slovak & Vogt (1979) from a distance–reddening relation for stars in a field near the nova but an improved determination of this relation by Duerbeck *et al.* (1980) gives a smaller distance for the nova, $d = 2.3 \pm 0.5$ kpc. It is noted by Gehrz *et al.* (1980) and by Gallagher *et al.* (1980) that a value of d smaller than that deduced from equation (3.3) is required if the maximum total luminosity L(max) is not to exceed the Eddington luminosity of the remnant, L(E). This will be discussed further in Section 4.3 where it will be shown that putting L(max) = L(E) gives $d = 2.2$ kpc $= 6.8 \times 10^{21}$ cm, which is the value we adopt. With this value we must note that Nova Cygni 1978 is underluminous in M_v(max) compared with, for example, Nova LMC 1977b.

3.3 EXPANSION VELOCITIES

We estimate the expansion velocity v of the nebular shell using the widths of the nebular emission lines in the optical spectra of Klare *et al.* and of the lines He II λ 1640 and N III] λ 1750 in an *IUE* high dispersion spectrum on $D = 60$. The maximum velocities deduced from the extreme widths of the lines give an average value of v(max) = 1370 km s^{-1}. The shapes of the profiles suggest that only a small fraction of the mass of the ejected shell has this maximum velocity. We estimate a velocity $\bar{v}$, which may be closer to an average expansion velocity, from the widths of the approximately flat-topped 'plateau' regions in the centres of the lines profiles. This gives $\bar{v} = 760$ km s^{-1}.

4 The total observed flux

4.1 FLUXES IN THE UV, OPTICAL AND IR REGIONS

We take the total observed flux, corrected for extinction, to be

$$F(\text{obs}) = F(\text{UV}) + F(\text{opt}) + F(\text{IR}), \tag{4.1}$$

where the *IUE* observations give the UV flux F(UV) for the wavelength range $1140 < \lambda < 3290$, the optical flux F(opt) is calculated for the range $3290 < \lambda < 12\,000$ using U, B, V magnitudes from Duerbeck *et al.* (1980) and fitting to blackbody distributions, and the infrared flux F(IR) for $1.2 < \lambda < 19.5\,\mu$m is obtained from observations by Joseph *et al.* (1981) and by Gehrz *et al.* (1980). Results for F(UV), F(opt) and F(IR) are shown separately on Fig. 3. Fig. 4 shows adopted smooth curves and deduced values of F(obs).

4.2 DISCUSSION OF THE FLUX

Let F(tot) be the total flux, including the unobserved regions of $\lambda < 1140$ Å and $\lambda > 19.5\,\mu$m. At earlier dates, up to $D = 16.5$ nearly all of the flux is in the observed region and we can put F(tot) = F(obs). It is seen that $\log F$(obs) has a maximum value of -6.5 on $D = 6$, falls to a value of -6.95 by $D = 13$ and then remains approximately constant to $D = 27$.

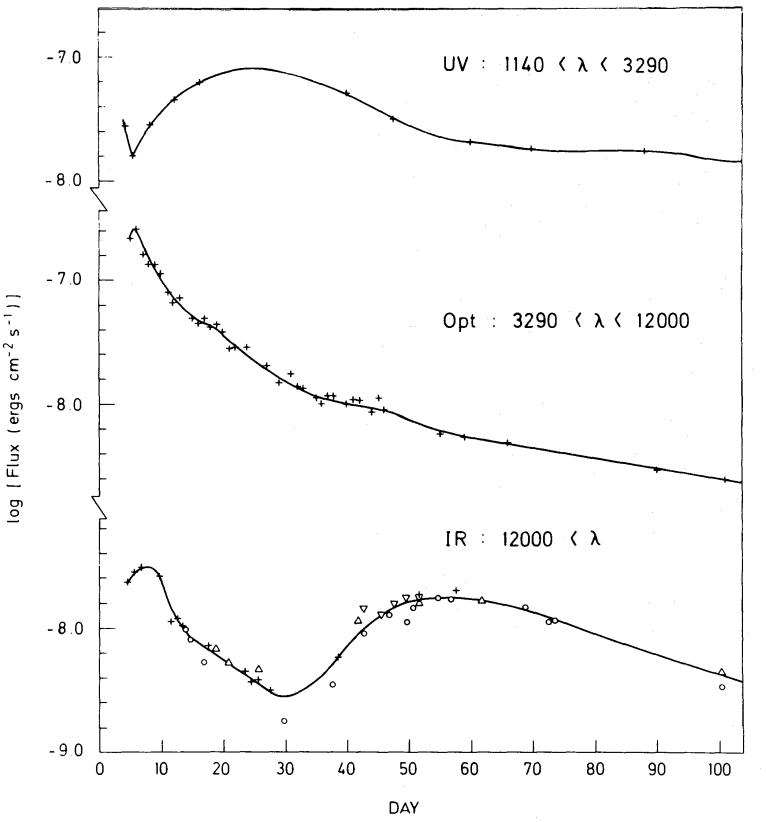

Figure 3. Total observed fluxes for Nova Cygni 1978 in the UV, optical and IR regions. UV observations from present work. Optical observations reported by Duerbeck *et al.* (1980). IR observations from Joseph *et al.* (1981), ▽; Gehrz *et al.* (1980), + (CIT), ○ (UW), △ (UM). The abbreviations CIT, UW and UM refer to the work of the three research groups described in the paper by Gehrz *et al.* (1980).

The period $D = 13$–27 will be referred to as the 'plateau region'. The subsequent drop in F(obs) may be due, initially, to an increase of radiation in the unobserved far UV, giving $F(\text{obs}) < F(\text{tot})$. For later dates, $D \gtrsim 100$, there can be little doubt about a real decrease of F(tot) with time.

The IR flux has a maximum on $D \simeq 55$. There is little, if any, evidence for a drop in the optical flux at this time, indicating that the dust does not form a shell which is optically thick at optical wavelengths. A similar conclusion has been reached by Gallagher *et al.* (1980), based on their *uvby* measurements. There is, on the other hand, some evidence for a dip in F(UV) during the period that F(IR) passes through its maximum. The IR emission will be discussed further in Section 11.

4.3 LUMINOSITIES

The luminosity is $L = 4\pi d^2 F$. With the total observed flux as given in Fig. 4 we obtain for the observed luminosity

$$L(\text{obs}) = \begin{cases} 1.0 \times 10^4 d^2 L_\odot \text{ for maximum value, } D = 6 \\ 3.5 \times 10^3 d^2 L_\odot \text{ for 'plateau' region, } D = 13\text{–}27, \end{cases} \tag{4.2}$$

with d in kpc.

The Eddington luminosity L(E) is obtained on equating the gravitational force produced by a central body of mass M to the force produced by electron-scattering radiation pressure.

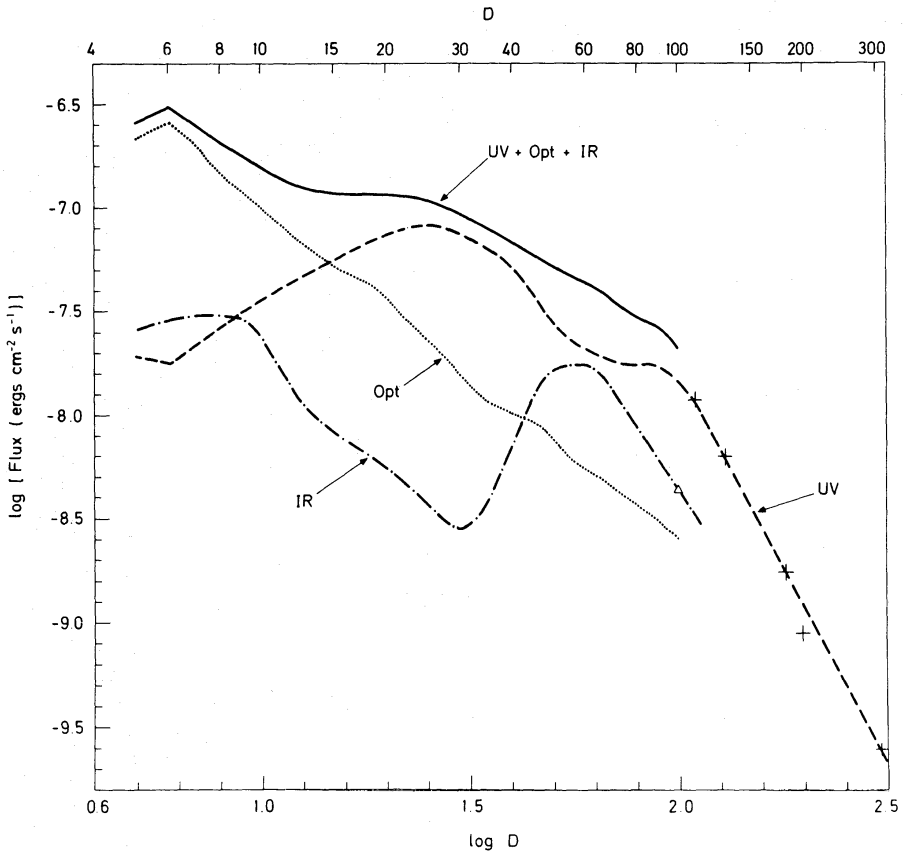

Figure 4. Adopted smooth curves for UV, optical and IR fluxes for Nova Cygni 1978 (wavelength ranges as in Fig. 3) and adopted total observed flux. Data points, additional to those used for Fig. 3, are: + from *IUE* observations; △ from Gehrz *et al.* (1980), UM.

This gives

$$L\,(\mathrm{E}) = 4\pi cGMm_{\mathrm{H}}\,\mu/\sigma_{\mathrm{T}}\,, \tag{4.3}$$

where m_{H} is the mass of the hydrogen atom, μ the mean molecular weight per free electron (in units of m_{H}) and $\sigma_{\mathrm{T}} = 8\pi e^4/(3m^2c^4)$ the Thomson scattering cross-section. From results which we shall give later (Section 7) for the ionic composition of the nebular shell we obtain $\mu \simeq 1.7$ and with this value of μ

$$L\,(\mathrm{E}) = 5.4 \times 10^4\,(M/M_\odot)\,L_\odot. \tag{4.4}$$

If the hot remnant has the mass of a white dwarf we can put $M = M_\odot$. At depths not far below the surface of its photosphere the ionic composition will not be very different from that which exists at later dates in the nebular shell. We therefore have $L\,(\mathrm{E}) \simeq 5 \times 10^4 L_\odot$ for the hot remnant. At the time when $F\,(\mathrm{obs})$ has its maximum value there will be little flux outside of the spectral region observed and the total luminosity is therefore $L\,(\mathrm{max}) = L\,(\mathrm{obs, max}) = 1.0 \times 10^4 d^2 L_\odot$. If we adopt $d = 3.6$ from equation (3.3) we obtain $L\,(\mathrm{max})/L\,(\mathrm{E}) = 2.6$. The total outward acceleration due to radiation pressure and gravity is $a = [L/L\,(\mathrm{E}) - 1]\,g$ with $g = GM/R^2$ which, with $M = M_\odot$ and $L/L\,(\mathrm{E}) = 2.6$ gives

$$a = 4 \times 10^4\,(R_\odot/R)^2\,\mathrm{km\,s^{-1}\,day^{-1}}. \tag{4.5}$$

For $D \simeq 6$ the radius of the photosphere will be of order $10–100\,R_\odot$ but we expect the source of radiant energy to be at a radius less than $1\,R_\odot$. Equation (4.5) gives an acceleration

at $R = R_\odot$ of $4 \times 10^4 \,\mathrm{km\,s^{-1}}$ per day, which is unacceptably large. We therefore prefer the distance $d = 2.2\,\mathrm{kpc}$ obtained on putting L (max) = L (E). A similar opinion is expressed by Gallagher *et al.*, who consider that a star with L significantly larger than L (E) would be in an unstable state and would give a light curve with a decline more rapid than that observed for Nova Cygni 1978.

5 Expressions for line emissivities and observed fluxes

5.1 RECOMBINATION LINES

For a recombination line of an ion A^{m+} and wavelength λ the emissivity per unit volume is

$$4\pi j(\lambda) = \left(\frac{hc}{\lambda}\right) \alpha_{\mathrm{eff}}(\lambda) N_{\mathrm{e}} N(A^{(m+1)+}), \tag{5.1}$$

where $\alpha_{\mathrm{eff}}(\lambda)$ is the effective recombination coefficient. Values of $\alpha_{\mathrm{eff}}(\lambda)$ which we have used for the lines C II λ 1335, C III λ 2297 and N IV λ 1718 are given in Table 3. The dielectronic mechanisms involved can be understood by considering the case of C II λ 1335. The

Table 3. Effective recombination coefficients, $\alpha_{\mathrm{eff}}(\lambda)$, for lines produced by dielectronic recombination. Values of $10^{12}\,\alpha_{\mathrm{eff}}(\lambda)$ with α_{eff} in $\mathrm{cm^3\,s^{-1}}$.

T_{e} ($\times 10^{-4}$) =	0.7	0.8	0.9	1.0	1.1	1.2	1.3	1.4	1.5
λ									
1335	–	5.72	5.17	4.72	4.33	3.99	3.71	3.45	–
2297	5.56	4.96	4.46	4.04	3.69	3.39	3.13	2.91	2.71
1718	4.33	4.39	4.34	4.24	4.11	3.95	3.75	3.63	3.47

(C^{2+} + e) system has a number of auto-ionizing states of the type $2s\,2p\,3d$ lying above the C^+ ionization limit but all within 0.69 eV of the limit. The states can radiate to C^+ $2s\,2p^2\,^2D$, the upper state for the λ 1335 line. We assume the radiative transition probabilities to be small compared with the probabilities of auto-ionization (Bates & Massey 1943; see also Seaton & Storey 1976); the populations of the auto-ionizing states are then given by the Saha equation and α_{eff} can be calculated once the radiative transition probabilities are known. The method of calculation is described more fully by Storey (1981), whose results are more accurate than those quoted here.

5.2 COLLISIONAL EXCITATION

For a line of A^{m+} excited by electron impacts the emissivity is given by

$$4\pi j(\lambda) = \left(\frac{hc}{\lambda}\right) q(\lambda, T_{\mathrm{e}}) N_{\mathrm{e}} N(A^{m+}), \tag{5.2}$$

where

$$q(\lambda, T) = \frac{8.63 \times 10^{-6} \Upsilon}{\omega_1 T_{\mathrm{e}}^{1/2}} \exp\left(-\frac{\Delta E}{k T_{\mathrm{e}}}\right) \mathrm{cm^3\,s^{-1}} \tag{5.3}$$

and where Υ is the collision strength integrated over the Maxwell distribution, ω_1 is the statistical weight of the ground state, and ΔE the excitation energy of the upper state. Equation (5.2) is valid if collisional de-excitation can be neglected.

5.3 COLLISIONAL DE-EXCITATION

If the de-excitation rate is much faster than the rate of radiative transitions, the upper state has a Boltzmann distribution and the emissivity is

$$4\pi j(\lambda) = \left(\frac{hc}{\lambda}\right)\frac{\omega_2}{\omega_1}\exp(-\Delta E/kT_e)A_{21}N(A^{m+}), \tag{5.4}$$

where A_{21} is the radiative transition probability.

5.4 LUMINOSITY AND OBSERVED FLUX

If there is no true absorption within the nova shell, the luminosity in a line is given by

$$L(\lambda) = \int 4\pi j(\lambda)\, dV, \tag{5.5}$$

where the integration is over the volume of the shell. The observed flux in the line, corrected for interstellar extinction, is

$$F(\lambda) = \frac{L(\lambda)}{4\pi d^2} \tag{5.6}$$

where d is the distance.

In addition to interstellar absorption there may be absorption due to dust within the nova shell, for which the optical depth is denoted by $\tau_d(\lambda)$. This may not have a normal 2200 Å feature and hence may not be included in the estimate of absorption obtained in Section 3.1. In Section 11 we shall give reasons for believing that $\tau_d(\lambda)$ is much less than unity. The condition $\tau_d \ll 1$ is not sufficient to ensure that there is negligible absorption in resonance lines, for which the photons are partially trapped by scattering. While scattering does not, in itself, lead to any loss of photons it may lead to an enhanced probability of absorption by dust. We shall assume that this is not of major importance, and that (5.4), (5.5) can be used for all of the observed lines. Some justification for this assumption will be given in Section 11.6.

5.5 DEFINITION OF THE QUANTITIES $n(A^{m+})$ AND $\mathcal{N}(A^{m+})$

For an ion A^{m+} with number density $N(A^{m+})$ we define

$$n(A^{m+}) = \int N(A^{m+})N_e\, dV/(4\pi d^2) \tag{5.7}$$

and

$$\mathcal{N}(A^{m+}) = \int N(A^{m+})\, dV/(4\pi d^2), \tag{5.8}$$

where the integrations are over the volume of the nebula. These quantities, as deduced from observations, do not depend on the distance d.

5.6 MEAN ELECTRON DENSITIES AND ELECTRON TEMPERATURES

A mean electron density $N_e(A^{m+})$ is defined by

$$N_e(A^{m+}) = \frac{\int N(A^{m+})N_e\, dV}{\int N(A^{m+})\, dV} = \frac{n(A^{m+})}{\mathcal{N}(A^{m+})}. \tag{5.9}$$

In defining mean electron temperatures we are mainly concerned with exponential factors which are sensitive to T_e. For an ion A^{m+} which has a state with excitation energy ΔE we define a mean temperature $T_e(A^{m+})$ by

$$\exp\left\{\frac{-\Delta E}{kT_e(A^{m+})}\right\} = \frac{\int \exp\left\{\frac{-\Delta E}{kT_e}\right\} N(A^{m+}) N_e \, dV}{\int N(A^{m+}) N_e \, dV} . \tag{5.10}$$

We generally neglect the temperature variation of quantities which do not depend exponentially on T_e.

5.7 EXPRESSIONS FOR LINE FLUXES

For a line in the spectrum of A^{m+} produced by recombination of $A^{(m+1)+}$ the flux is

$$F(\lambda) = \left(\frac{hc}{\lambda}\right) \alpha_{\text{eff}}(\lambda) \, n(A^{(m+1)+}) , \tag{5.11}$$

where the effective recombination $\alpha_{\text{eff}}(\lambda)$ varies slowly with T_e and has been taken outside of the integral.

For lines excited by collisions we use mean temperatures defined by (5.10). The flux is

$$F(\lambda) = \left(\frac{hc}{\lambda}\right) q\,[\lambda, T_e(A^{m+})] \, n(A^{m+}) \tag{5.12}$$

if the emissivity is given by (5.2) and

$$F(\lambda) = \left(\frac{hc}{\lambda}\right) \frac{\omega_2}{\omega_1} \exp\left\{\frac{-\Delta E}{kT_e(A^{m+})}\right\} A_{21} \, \mathcal{N}(A^{m+}) \tag{5.13}$$

if the emissivity is given by (5.4).

Let us define

$$n(A) = \sum_m n(A^{m+}) , \tag{5.14}$$

where the sum is over all ionization stages which give significant contributions. For any two elements A and B the chemical abundance ratio is

$$\frac{N(A)}{N(B)} = \frac{\sum_m N(A^{m+})}{\sum_m N(B^{m+})} . \tag{5.15}$$

Assuming this ratio to be independent of position we have

$$\frac{n(B)}{n(A)} = \frac{N(B)}{N(A)} . \tag{5.16}$$

6 Determination of electron temperatures and electron densities

6.1 ELECTRON TEMPERATURES

Electron temperatures T_e(C III), T_e(C IV) and T_e(N V) are deduced from ratios (λ 1335)/(λ 1909), (λ 2297)/(λ 1549) and (λ 1718)/(λ 1240) of fluxes in lines produced by dielectronic recombination to fluxes in lines produced by collisional excitation.

Table 4. Electron temperatures, T_e (C III), T_e (C IV) and T_e (N V).

Ion	$D = 70$	88	110	128	180	198	304
C III	9 220 ± 30	9 810 ± 60	9 730 ± 50	9 640 ± 70	9 500 ± 190	8 930 ± 80	8 440 ± 60
C IV	10 700 ± 200	11 300 ± 200	12 900 ± 700	12 200 ± 800	11 500 ± 900	11 100 ± 300	–
N V	13 300 ± 600	15 100 ± 800	15 300 ± 400	14 800 ± 1000	16 200 ± 1400	14 400 ± 300	13 700 ± 400

The method can be understood by considering the case of (λ 1335)/(λ 1909) for which the ratio of fluxes is given by, using (5.11) and (5.12)

$$\frac{F(1335)}{F(1909)} = \frac{(1909)}{(1335)} \frac{\alpha_{\rm eff}(1335)}{q[1909, T_e(\text{C III})]} \tag{6.1}$$

which is used to calculate T_e (C III).

Results obtained for T_e (C III), T_e (C IV) and T_e (N V) are given in Table 4. The trend is that higher values of T_e are obtained for the more highly ionized systems. A similar trend is found from the nebular spectra of various other objects. For ions other than C III, C IV and N V we use values of T_e interpolated as functions of ionization potential.

6.2 ELECTRON DENSITIES

We put the optical fluxes of Klare *et al.* on the absolute scale used for the UV fluxes using the methods described in Section 2.2. We estimate electron densities $N_e(N^+)$ and $N_e(O^{2+})$ from the flux ratios (N II λ 2140)/(N II λ 5755) and (O III λ 1663)/(O III λ 5007) of intercombination lines to forbidden lines. For $D = 88$ we obtain $N_e(N^+) = N_e(O^{2+}) \simeq 8 \times 10^7 \text{cm}^{-3}$. At this density it is a good approximation to neglect collisional de-excitation for the intercombination lines and to use Boltzmann distributions for the upper levels of the forbidden lines.

We therefore conclude that

$$N_e(A^{m+}) = N_e(O^{2+}) = 8 \times 10^7 \text{cm}^{-3} \text{ for } D = 88 \tag{6.2}$$

with $N_e(A^{m+})$ defined by (5.9).

7 Abundances

We obtain values of $n(A^{m+})$ using fluxes corrected for extinction, equations (5.8), (5.9) and (5.11), and values of T_e obtained using methods described in Section 6.1.

7.1 RESULTS FROM THE UV LINES

Table 5 gives values of $n(A^{m+})/n(He^{2+})$, where A = C, N and O. These are deduced from fluxes in UV lines relative to the flux in He II λ 1640. Values of $n(O^+)$ are deduced from the forbidden line [O II] λ 2470 assuming $N_e(O^+) = 2 \times 10^8$ for $D = 70$ and 8×10^7 for $D = 88$.

For C we observe three ionization stages; for N we observe four; and for O we observe four on $D = 88$ and 110 and less on other dates. We plot histograms of $n(A^{m+})/n(He^{2+})$ against ionization potentials and estimate values of $n(A^{m+})/n(He^{2+})$ for ionization stages which are not observed; this gives the numbers shown in brackets in Table 5. We recognize the approximations involved in this procedure. The ionization equilibria do not depend only

Table 5. Values of $n(A^{m+})/n(He^{2+})$. Figures in brackets are estimated values.

A^{m+}	$D = 70$	88	110	128	180	198	304
C^{+}	0.08	0.07	0.16	0.22	0.09	0.22	(0.20)
C^{2+}	0.29	0.24	0.25	0.28	0.20	0.36	0.27
C^{3+}	0.06	0.10	0.04	0.06	0.07	0.11	0.08
C^{4+}	(0.07)	(0.07)	(0.07)	(0.09)	(0.06)	(0.08)	(0.06)
C	0.50	0.48	0.52	0.65	0.42	0.77	0.61
N^{+}	0.29	0.25	0.40	0.37	0.24	0.24	(0.20)
N^{2+}	0.88	0.74	0.59	0.71	0.56	0.92	0.73
N^{3+}	0.29	0.40	0.17	0.21	0.33	0.56	0.43
N^{4+}	0.03	0.03	0.05	0.07	0.03	0.08	0.05
N	1.49	1.42	1.21	1.36	1.16	1.80	1.41
O^{+}	0.33	0.18	0.22	(0.22)	(0.22)	(0.22)	(0.22)
O^{2+}	0.55	0.49	0.34	0.48	0.43	0.61	0.50
O^{3+}	0.38	0.44	0.25	0.45	0.42	0.55	0.65
O^{4+}	(0.03)	0.03	0.05	(0.04)	0.04	(0.04)	(0.04)
O	1.29	1.14	0.80	1.19	0.93	1.24	1.23
He	(4.60)	(5.30)	(6.70)	(5.90)	(4.20)	(3.60)	(3.70)

on ionization potentials; in a more complete treatment one would have to take account of variations in individual photo-ionization cross-sections and in recombination rates, including dielectronic recombination and charge-exchange processes. Fortunately, for C, N and O, observations give us directly the abundances in the ionization stages of maximum abundance.

The last row of Table 5 gives approximate values of $n(\mathrm{He})/n(\mathrm{He}^{2+})$ estimated using the approximate procedure described in the previous paragraph. The best value to adopt for these ratios will be discussed further in Sections 7.2 and 8.

Table 5 includes values of $n(\mathrm{A})/n(\mathrm{He}^{2+})$ for A = C, N and O; these are obtained on summing the results for the ion abundances. The relative abundances of C, N and O, $N(A)/[N(\mathrm{C}) + N(\mathrm{N}) + N(\mathrm{O})]$, are given in Table 6; they are obtained using equation (5.14) and the results of Table 5. It is seen that similar results are obtained on different dates. The table includes mean values of the ratios.

Table 7 gives absolute values of $n(\mathrm{He}^{2+})$ and $n(\mathrm{N})$, the former being obtained from absolute He II λ1640 fluxes and the latter being given because nitrogen is observed in all ionization stages contributing significantly to the total abundance.

Table 6. Relative abundances of C, N, and O.

	$N(A)/[N(\mathrm{C}) + N(\mathrm{N}) + N(\mathrm{O})]$							
A	$D = 70$	88	110	128	180	198	304	Mean
C	0.15	0.16	0.21	0.20	0.17	0.20	0.19	0.18 ± 0.02
N	0.45	0.47	0.48	0.43	0.46	0.47	0.43	0.46 ± 0.02
O	0.39	0.38	0.31	0.37	0.37	0.33	0.38	0.36 ± 0.03

Table 7. Values of $n(He^{2+})$ and $n(N)$, (in units of cm^{-5}), and of $D^3 n(N)$ and $D^3 n(He^{2+})$ (D in days).

D	$10^{-12} n(He^{2+})$	$10^{-12} n(N)$	$10^{-19} D^3 n(He^{2+})$	$10^{-19} D^3 n(N)$
70	43.7	57.6	1.50	1.97
88	24.9	35.4	1.70	2.41
110	14.7	17.8	1.96	2.37
128	7.4	10.1	1.61	2.12
180	2.21	2.56	1.29	1.49
198	1.30	2.34	1.01	1.82
304	0.50	0.71	1.40	1.99

7.2 RESULTS FROM THE OPTICAL LINES

We use the optical observations of Klare *et al.* (1981) to determine the helium ionization equilibrium and the He/H abundance ratio.

From fluxes in the He II λ 4686 relative to Hβ λ 4861 and in He I λ 5876 relative to Hα λ 6563 we estimate values of $n(He^{2+})/n(H^+)$ and $n(He^+)/n(H^+)$. We obtain $n(He^{2+})/n(H^+) = 0.014$ and $n(He^+)/n(H^+) = 0.103$ for $D = 75$ and $n(He^{2+})/n(H^+) = 0.026$ for $D = 102$. The results for $D = 75$ give

$$\frac{N(He)}{N(H)} = 0.12 \tag{7.1}$$

which is the value we shall adopt. The UV observations suggest that there is not much change in the ionization equilibrium between $D = 75$ and 102 but the optical observations suggest that there may be some change in the He^{2+}/H^+ ratio.

The UV observations give abundances relative to He^{2+}. In order to obtain abundances relative to hydrogen we require values of $n(He^{2+})/n(H^+)$. Using (7.1) we have

$$\frac{n(He^{2+})}{n(H^+)} = 0.12 \frac{n(He^{2+})}{n(He)} . \tag{7.2}$$

Table 8 gives approximate values of $n(He^{2+})/n(H^+)$ obtained from the UV observations, using (7.2) and results from the last row of Table 5. It is seen that there are discrepancies by factors of about two between these results and those from the optical observations. These are no greater than would be expected from difficulties in optical calibration and approximations used in the treatment of the ionization equilibria. Fortunately an independent estimate of $n(He^{2+})/n(H^+)$ can be obtained from the UV continuum; results for $D = 70$, to be discussed in Section 8, give

$$\frac{n(He^{2+})}{n(H^+)} = 0.014 \text{ for } D = 70 \tag{7.3}$$

in good agreement with the optical results for $D = 75$.

Table 8. Approximate values of $n(He^{2+})/n(H^+)$ obtained using (7.1) and estimates of the ionization equilibrium from the results of Table 5.

D =	70	88	110	128	180	198	304
$\frac{n(He^{2+})}{n(H^+)}$ =	0.026	0.023	0.018	0.020	0.029	0.033	0.032

Table 9. Adopted abundances for Nova Cygni 1978 and for the Sun.

A	$N(A)/N(H)$		$X(A)$	
	Nova	Sun	Nova	Sun
H	1.00	1.00	0.47	0.70
He	0.12	0.10	0.22	0.28
C	0.008	4.7×10^{-4}	0.04	0.0039
N	0.021	9.8×10^{-5}	0.14	0.0010
O	0.017	8.3×10^{-4}	0.13	0.0094

7.3 FINAL RESULTS FOR ABUNDANCES OF HELIUM, CARBON, NITROGEN AND OXYGEN

We use the following results: (i) $N(\mathrm{He})/N(\mathrm{H})$ given by (7.1); (ii) $N(A)/[N(\mathrm{C})+N(\mathrm{N})+N(\mathrm{O})]$ from the mean results of Table 6; (iii) $[n(\mathrm{C})+n(\mathrm{N})+n(\mathrm{O})]/n(\mathrm{He}^{2+})$ for $D=70$ from Table 5; (iv) $n(\mathrm{He}^{2+})/n(\mathrm{H}^{+})=0.014$ for $D=70$ as discussed in Section 7.2. Table 9 gives our adopted abundances, by number and by mass fraction. Results for Nova Cygni 1978 are compared with results of Lambert (1978) for the Sun.

We note that the relative abundances of C, N, O nuclei, $\rho(A)\equiv N(\mathrm{A})/[N(\mathrm{C})+N(\mathrm{N})+N(\mathrm{O})]$ with $A=$ C, N or O, are more accurate than the deduced abundances relative to H. It is seen from Table 6 that there is good agreement between results for $\rho(A)$ obtained on different dates. The standard deviations from the means for seven dates, given in the last column of Table 6, are no larger than 10 per cent. The values of $\rho(A)$ are also insensitive to assumed values of electron temperature, T_e.

8 The continuum spectrum

Our best observations for the continuum and weak lines, for $D=70$, have been discussed in Sections 2.2 and 3.1. We now consider the interpretation of these observations.

8.1 THE NEBULAR CONTINUUM

We use the absolute He II λ 1640 flux, the relative abundances from Table 9, the ionization equilibrium for $D=70$ from Table 5 and equation (7.3), and electron temperatures interpolated from Table 4. We compute the continuum emission due to recombination and free–free processes using hydrogenic cross-sections. Threshold wavelengths for recombination processes are determined using experimental energy levels, with some grouping of thresholds which come close together. We do not include the H $2s\rightarrow 1s$ two-photon continuum since the $2s$ state is collisionally de-excited for N_e greater than about $10^4\,\mathrm{cm}^{-3}$.

8.2 THE STELLAR CONTINUUM

We assume the star to radiate like a blackbody at temperature T_s and to subtend an angle of θ radians at the Earth. The total flux at the distance of the Earth is

$$F(\mathrm{star})=\theta^2\sigma_S T_s^4, \qquad (8.1)$$

where $\sigma_S = (2k^4\pi^5)/(15h^3c^2)$ is the Stefan–Boltzmann constant. Let F_λ (star) be the corresponding flux per unit wavelength. Then, from $F_\lambda = \theta^2 \pi B_\lambda (T_s)$, we obtain

$$\lambda F_\lambda (\text{star}) = \frac{15}{\pi^4} \frac{u^4}{\exp(u) - 1} F(\text{star}), \tag{8.2}$$

where $u = (hc)/(\lambda k T_s)$.

Let F(obs) be the total observed radiation, corrected for extinction. The observations are made for all wavelengths greater than 1140 Å. In Section 11 we shall show that, for D = 70, most of the radiation in the Lyman continuum ($\lambda < 912$ Å) is probably absorbed by photo-ionization processes or by dust. Energy absorbed by dust will be re-radiated in the IR and included in F(obs). A substantial part of the energy absorbed by photo-ionization will be re-emitted at wavelengths for which the flux is observed. We do not observe radiation in the hydrogen Ly α line or in resonance lines with $\lambda < 1140$ Å, but in Section 11 we shall show that a substantial part of the energy in these lines is probably absorbed by dust and re-emitted in the IR. For this reason we put F(star) = F(obs) in equation (8.2) where, for D = 70, F(obs) = 3.9×10^{-8} erg cm^{-2} s^{-1}. The error in F(star) is probably not larger than 30 per cent.

Having fixed F(star), F_λ (star) calculated from equation (8.2) is sensitive to T_s (approximately proportional to T_s^{-3}). Our procedure is therefore to vary T_s so as to obtain a best fit to the observed flux.

8.3 COMPARISON OF CALCULATED AND OBSERVED FLUX F_λ

Fig. 5 shows, for D = 70: the observed flux F_λ; the calculated nebular continuum flux; the stellar flux calculated assuming T_s = 140 000 K; and the sum of the calculated nebular and

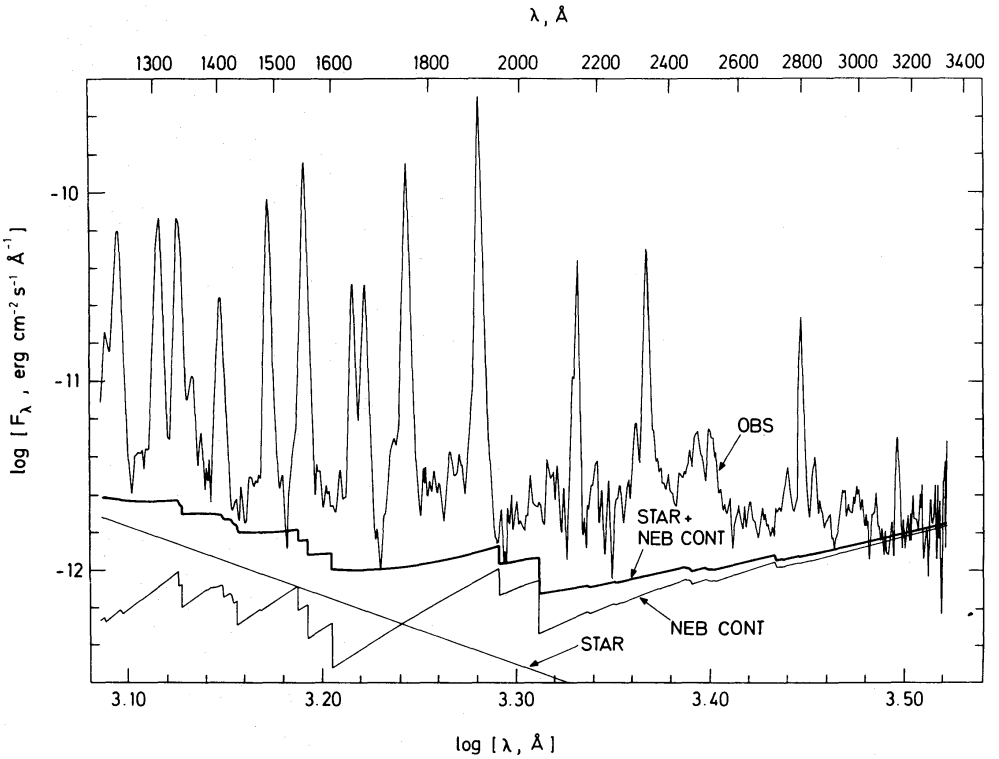

Figure 5. The logarithm of the observed flux for D = 70, and logarithms of calculated fluxes for: nebular continuum; stellar remnant; and nebular continuum plus stellar remnant.

stellar fluxes. Two empirical adjustments have been made, the choice of 0.014 for the ratio $n(He^{2+})/n(H^+)$ and the choice of T_s.

The observed flux is plotted for wavelengths out to 3320 Å. At the longest wavelengths considered the spectra are noisy due to a rapid decrease in the *IUE* sensitivity. Towards the long wavelength end of Fig. 5 the calculated continuum is due almost entirely to the hydrogen Balmer continuum and, for a given value of the flux in He II λ 1640, its strength is inversely proportional to the ratio $n(He^{2+})/n(H^+)$. Our adopted value is seen to give good agreement with the observations. We recall that the value used is consistent with results deduced from observation of hydrogen lines in the optical but that the latter results are uncertain by factors of about two due to difficulties in calibration.

Due to their high abundances, the ions of C, N and O give important contributions to the nebular continuum at shorter wavelengths. It follows that we can also expect to have contributions to the observed flux from large numbers of weak recombination lines. The calculated continuum shows a number of emission edges. To the longwave side of each edge there will be a series of lines, converging to the edge, and if such lines are unresolved they will give an apparent continuum which joins smoothly to the continuum on the shortwave side of the edge. We would therefore not expect sharp edges to be seen in the observed spectra. We note that the observed flux shows a number of rather deep minima. With the exception of the noisy region of $\lambda > 3000$ Å, we consider that the observed minimum fluxes are probably real (examination of the raw data shows the signal to be well above the background level, and the minima are found to be reproducible on different dates). The minima probably correspond to regions which happen to be free of lines and the minimum observed fluxes probably come close to the true continuum level. It is seen from Fig. 5 that they come close to the calculated continuum level.

Our adopted value of 140 000 K for T_s is chosen to give a best fit between observed and calculated spectra. If T_s is varied by more than ± 10 000 K the fit is significantly less good.

9 The radius of the stellar remnant

The determination of T_s will be discussed further in Section 13.1 where it will be shown that the best estimate is provided by the continuum fit. Taking $F(\text{star}) \simeq F(\text{obs}) = 3.9 \times 10^{-8}$ erg cm^{-2} s^{-1} and $T_s = 140\,000$ K we obtain, from equation (8.1), $\theta = 1.34 \times 10^{-12}$ rad. With a distance of 2.2 kpc this gives the star radius to be $R_s = 0.13\,R_\odot$ on $D = 70$.

The accuracy of this result can be assessed as follows. At $\lambda \simeq 1400$ Å we have $\log(\lambda) = 3.15$, $u = 0.73$ and $\exp(u) - 1 = 1.08$. If we put $\exp(u) - 1 = u$, corresponding to the Rayleigh–Jeans limit, (8.2) gives $F_\lambda(\text{star}) \propto \theta^2 T_s$. Since $F(\text{star}) \propto \theta^2 T_s^4$ we can eliminate T_s to obtain $\theta \propto [F_\lambda(\text{star})]^{2/3}/[F(\text{star})]^{1/6}$. This is seen to be very insensitive to errors in $F(\text{star})$ and not too sensitive to errors in $F_\lambda(\text{star})$.

10 Lines produced by fluorescence

10.1 THE O III BOWEN LINES

The O III Bowen lines $2p\,3d\,^3P_2^0 \rightarrow 2p\,3p\,^3S$ λ 3133 and $2p\,3d\,^3P_2^0 \rightarrow 2p\,3p\,^3D_3$ λ 2837 are observed in the Nova spectra. They are produced by excitation of O III $2p^2\,^3P_2 \rightarrow 2p\,3d\,^3P_2^0$ λ 303.80 by absorption of He II Lyα λ 303.78. Let R be the fraction of He II Lyα photons which are converted to photons in Bowen cascades. Using results of Saraph & Seaton (1980) together with the He II (λ 1640)/(λ 4686) ratio from Seaton (1978) we obtain

$$R = 2.2\,F(3133)/F(1640) \qquad (10.1)$$

The observed ratio $F(3133)/F(1640)$ shows some tendency to increase with time; the mean value for day $D = 70$–198 is 0.46 ± 0.07 giving

$$R = 0.8 \pm 0.1 . \qquad (10.2)$$

For planetary nebulae the value of R deduced from observations is about 0.5, in good agreement with theoretical values obtained from solutions of the radiative transfer problem (Weymann & Williams 1969; Harrington 1972). For the nova the transfer problem may be more complicated due to possible large velocity gradients, which will tend to reduce R. On the other hand, the much higher oxygen abundance in the nova will tend to give a larger value of R. A study of the transfer problem for the nova would be of interest. The one conclusion which we can reach, in the absence of such a study, is that the number of scatterings of He II Lyα photons must be very large (if each He II Lyα photon is absorbed only once by O III one obtains $R = 0.019$).

10.2 THE O I λ 1303 LINE

The O I line $2p^3\,3s\,^3S^0 \rightarrow 2p^4\,^3P$ λ 1303 is produced by a fluorescent mechanism involving excitation of O I $2p^4\,^3P_2 \rightarrow 2p^3\,3d\,^3D^0$ λ 1025.77 by H Lyβ λ 1025.72, followed by cascades $3d\,^3D^0 \rightarrow 3p\,^3P$ λ = 1.13 μm and $3p\,^3P \rightarrow 3s\,^3S^0$ λ 8446. A study of the radiative transfer problem for Lyβ and O I would also be of interest.

Fluxes in the O I lines at 1.13 μm and 8446 Å have not, to our knowledge, been measured for Nova Cygni 1978. Such measurement would be of value in providing a means of determining the extinction, since the relative emission intensities are known for the three lines, 1.13 μm, 8446 Å and 1303 Å. It would be necessary to allow for some reduction in the λ 1303 flux due to interstellar line absorption but this should not be difficult since the interstellar lines will be much narrower than the emission line from the nova, and they can be measured on high dispersion spectra.

11 The thermal infrared emission

11.1 OBSERVATIONS OF THE THERMAL INFRARED FLUX

In Section 4 we considered the IR flux, F(IR), defined as the total flux for $\lambda > 1.2\,\mu$m. This includes contributions from free–free emission (and possibly also IR line emission), which the observations of Gehrz *et al.* (1980) showed to be dominant until $D = 30$. Subsequently the IR spectra showed evidence for thermal infrared emission by dust. This emission, which we shall refer to as the TIR emission, produced maxima in the IR spectra at $\lambda \simeq 3.7\,\mu$m, characteristic of thermal radiation at a temperature of about 1000 K. Let F_λ(TIR) be the TIR flux per unit wavelength, F(TIR) the total TIR flux. Gehrz *et al.* consider $(\lambda F_\lambda)_{\max}$ which is defined as the maximum value of λF_λ(TIR) as a function of λ. The relation between λF_λ(TIR) and F(TIR) has the form of equation (8.2). From this it follows that $F(\mathrm{TIR}) = 1.36\,(\lambda F_\lambda)_{\max}$.

We consider the possibility that the TIR emission is caused by dust which is heated by absorption of radiation in UV resonance lines. Such radiation is partially trapped by scattering in the line, which enhances the probability of its being absorbed by the dust.

11.2 TIME VARIATION OF NEBULAR AND TIR RADIATION

We compare the time variation of the TIR flux with that of the flux in a nebular line. For this purpose we choose a line which is well observed on many dates and for which the

emissivity is insensitive to the electron temperature and to possible changes in the ionization equilibrium. Our choice is the dielectronic recombination line C II λ 1335.

Fig. 6 shows, as functions of day number, F(TIR) from Fig. 4(a) of Gehrz *et al.* (1980) and $F(1335) \times 10^2$. Unfortunately we do not have observations of $F(1335)$ between $D = 16.5$ and 38 but we do have an upper limit for $D = 16.5$, which is plotted. It is seen that F(TIR) and $F(1335)$ both have maxima around $D = 60$. At later dates $F(1335)$ declines as D^{-3}. The decline of F(TIR) is similar but may be a little faster.

11.3 THE LYα FLUX

The Lyα flux is, assuming case B,

$$F(\text{Ly}\alpha) = (h\nu)_{\text{Ly}\alpha}\, \alpha_B(\text{H}^0)\, n(\text{H}^+) \tag{11.1}$$

where $\alpha_B(\text{H}^0)$ is the coefficient for recombination to all excited states of hydrogen. For $T_e = 10^4$ K, $\alpha_B(\text{H}^0) = 2.58 \times 10^{-13}\,\text{cm}^{-3}\,\text{s}^{-1}$. With the abundances of Table 9 we have $n(\text{H}^+) = 56\,n(\text{N})$. Table 7 shows that $D^3 n(\text{N})$ is approximately constant for $D \geqslant 70$. We adopt a mean value of $D^3 n(\text{N}) = 2.09 \times 10^{19}\,\text{cm}^{-5}\,\text{day}^3$. This gives

$$\log F(\text{Ly}\alpha) = -2.30 - 3 \log D \tag{11.2}$$

which is plotted on Fig. 6. It is seen that F(Lyα) is a little larger than F(TIR).

11.4 OTHER UV RESONANCE LINES

Assuming $n(\text{He}^{2+}) = 0.014\,n(\text{H}^+)$ we obtain $F(\text{He II Ly}\alpha) = 0.34 \times F(\text{H Ly}\alpha)$. Assuming that all recombinations to He I triplet states are eventually followed by collisional transitions to singlet states we obtain $F(\text{He I}\ 2^1P \rightarrow 1^1S) = 0.23\,F(\text{H Ly}\alpha)$. For resonance lines of C, N and O produced by recombination, approximate calculations using the ion abundances of

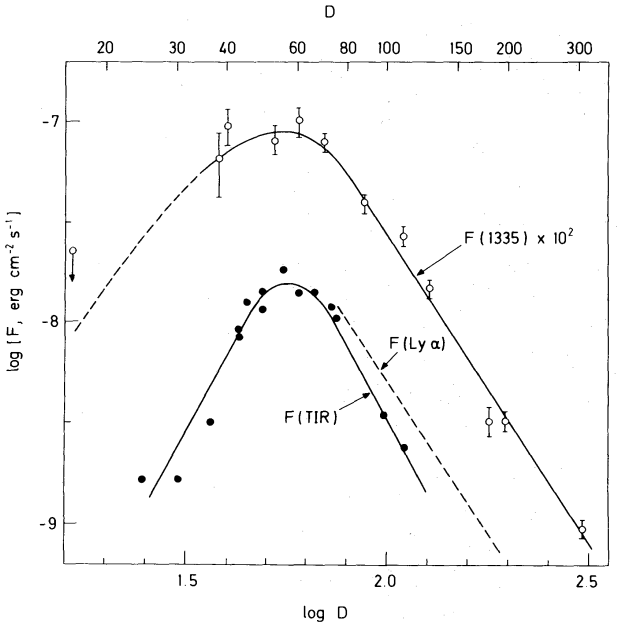

Figure 6. The thermal infrared flux, F(TIR), from Gehrz *et al.* (1980); the observed flux in C II λ 1335, multiplied by 10^2; and the estimated Lyα flux.

Table 5 give, as a rather crude estimate, F(CNO resonance lines) $\simeq 0.7F$(H Lyα). For C IV λ1549, the strongest UV resonance line excited by collisions, we have F(C IV λ1549) $\simeq 0.17F$(H Lyα). Adding these contributions we obtain

$$F(\text{UV resonance lines}) \simeq 3.0F(\text{TIR}) \tag{11.3}$$

11.5 DISCUSSION OF THE TIR EMISSION

It follows from equation (11.3) that one can explain the observed TIR emission if one assumes that about 30 per cent of the UV resonance line radiation is absorbed by dust.

The theory of Hummer & Kunasz (1980) can be used to estimate the efficiency of absorption of resonance line radiation by dust, for the case of a nebula without velocity gradients. Applying this theory to Nova Cygni 1978 we obtain efficiencies larger than 30 per cent for dust optical depths τ_D of about 0.1. Although we do not attempt a detailed calculation of the extent to which velocity gradients will reduce the efficiency, we note that our discussion of the O III Bowen lines in Section 10.1 shows that photons in resonance lines will be scattered many times before they escape. We therefore think it likely that the dust is heated by UV resonance line radiation.

Our work lends support to the view that the onset of TIR emission is due, not to the formation of a dust shell, but to the more efficient heating of pre-existing dust when there is more radiation in the far UV region. Bode & Evans (1980) suggest that the absorption is by spherical graphite grains which have two broad absorption features, centred at 2100 and 800 Å. Absorption of continuum radiation by such particles would not explain the heating of dust in Nova Cygni 1978 because the amount of continuum radiation within the region of the absorption features would be too small. We also note that the λ2200 feature which is observed is almost certainly of interstellar origin, since the value of $E(B-V)$ which we deduce from this feature is in fairly close agreement with the value deduced from a study of interstellar absorption lines (see Section 3.2).

11.6 DUST ABSORPTION FOR OBSERVED UV RESONANCE LINES

It was assumed, in Section 5.4, that one could neglect internal dust absorption for the observed UV resonance lines. We can now give two arguments which indicate that this assumption does not lead to major errors.

The first is that observations of the TIR emission suggest that the absorption for all resonance lines is about 30 per cent. The amount for the observed lines is likely to be less, since the dust opacity probably increases with decreasing wavelength.

Our second argument involves considering the errors in the determination of electron temperatures which would arise if there were a large amount of dust absorption. The temperatures T_e(C III), T_e(C IV) and T_e(N V) are determined using equations of the type (6.1) and the ratios (λ1335)/(λ1909), (λ2297)/(λ1549) and (λ1718)/(λ1240) of fluxes in recombination lines to fluxes in collisionally excited lines. The values of T_e given in Table 4 were obtained neglecting dust absorption. If there is dust absorption in the resonance lines λ1335, λ1549 and λ1240, our value of T_e(C III) is overestimated and our values of T_e(C IV) and T_e(N V) are underestimated. The trend of our values of T_e, from Table 4, is such that larger values of T_e are obtained for the more highly ionized systems which, as we have noted, is consistent with the trend deduced from nebular spectra of other objects. If there were important effects of dust absorption in λ1335, λ1549 and λ1240, the temperatures corrected for such effects would show larger differences between T_e (C III) on the one

hand and T_e (C IV), T_e (N V) on the other. Such larger differences would not be expected, and we therefore conclude that absorption in resonance lines is not large enough to give major errors in our interpretation of the line fluxes, although we cannot exclude the possibility of there being some significant absorption.

12 Mass of the ejected shell

12.1 OPTICAL DEPTHS FOR IONIZING RADIATION

During the initial nebular phase, the shell is certainly optically thick for ionizing radiation; so long as the temperature of the remnant is low, and increasing with time, the number of ionizations in the shell is equal to the number of stellar quanta beyond the Lyman limit. If, at later dates, it is assumed that the remnant has a constant temperature and luminosity, the nebula will eventually become optically thin since the number of recombinations will decrease due to expansion of the shell. We consider the quantity

$$n(\mathrm{N}) = \sum_{m \geqslant 1} n(\mathrm{N}^{m+}) \tag{12.1}$$

(see equations 5.7 and 5.14), choosing nitrogen because all contributing ionization stages are observed. It will be shown in Section 12.2 below that, for an optically thin expanding nebula, $n(\mathrm{N})$ will be proportional to D^{-3}. This behaviour is observed for later dates, as shown by Table 7, suggesting that the shell is optically thin. This argument, however, is not conclusive, as may be shown by considering the behaviour of $n(\mathrm{He}^{2+})$ which is proportional to the number of recombinations of He^{2+}. Table 7 shows that $n(\mathrm{He}^{2+})$ also behaves approximately like D^{-3}. The optical depth for photo-ionization of He^{+} can be estimated using the observed He^{+} abundance; we find that the threshold optical depth is greater than 10^3 during the entire period for which observations of the nebular spectra were made. It follows that $n(\mathrm{He}^{2+})$ is determined by the number of quanta available for ionization of He^{+}, and that this number must decrease in such a way that $n(\mathrm{He}^{2+})$ has a variation with time which mimics the behaviour which would be expected for an expanding nebula which is optically thin for ionization of He^{+}.

12.2 EXPANSION OF THE NEBULAR SHELL

Since nitrogen is observed in all ionization stages having significant abundance, we consider the number of ionized nitrogen atoms, $4\pi d^2 \mathcal{N}(\mathrm{N})$ where

$$\mathcal{N}(\mathrm{N}) = \sum_{m \geqslant 1} \mathcal{N}(\mathrm{N}^{m+}) . \tag{12.2}$$

Let $4\pi d^2 \delta\mathcal{N}(\mathrm{N})$ have velocity between v and $v + \delta v$ and put

$$\delta\mathcal{N} = \mathcal{N} f(v)\, dv \tag{12.3}$$

with

$$\int f(v)\, dv = 1 . \tag{12.4}$$

We assume atoms with velocity between v and $v + \delta v$ to be in a shell with radii between $r = vt$ and $r + \delta r = (v + \delta v)t$. The volume of the shell is

$$\delta V = 4\pi r^2 \delta r = 4\pi t^3 v^2 \delta v \tag{12.5}$$

and the number of atoms per unit volume at radius r and time t is

$$N(\mathrm{N};r,t) = 4\pi d^2\,\mathcal{N}(\mathrm{N}) \times \frac{f(v)}{4\pi t^3 v^2}\,. \tag{12.6}$$

Let us now consider

$$4\pi d^2 n(\mathrm{N}) = \int N(\mathrm{N}) N_e\, dv\,. \tag{12.7}$$

If we assume $N_e/N(\mathrm{N})$ to be the same at all points we obtain

$$4\pi d^2 n(\mathrm{N}) = \left(\frac{N_e}{N(\mathrm{N})}\right) \int [N(\mathrm{N})]^2\, dV \tag{12.8}$$

and using (12.5), (12.6),

$$n(\mathrm{N}) = 4\pi d^2 \left(\frac{N_e}{N(\mathrm{N})}\right) \frac{[\mathcal{N}(\mathrm{N})]^2}{4\pi t^3} \int \left[\frac{f(v)}{v}\right]^2 dv\,. \tag{12.9}$$

If the shell is fully ionized, $4\pi d^2 \mathcal{N}(\mathrm{N})$ is equal to the total number of nitrogen atoms in the shell and is independent of time. In this case, $n(\mathrm{N})$ varies with time as t^{-3}, as discussed in Section 12.1.

12.3 USE OF ESTIMATES OF ELECTRON DENSITY

We define a mean electron density, $N_e(\mathrm{N})$, by

$$n(\mathrm{N}) = N_e(\mathrm{N})\,\mathcal{N}(\mathrm{N}) \tag{12.10}$$

and consider $D = 88$. In Section 6.2 we obtained $N_e(\mathrm{N}^+) \simeq N_e(\mathrm{O}^{2+}) \simeq 8 \times 10^7\,\mathrm{cm}^{-3}$. We take $N_e(\mathrm{N}) = 8 \times 10^7$ and $n(\mathrm{N}) = 3.5 \times 10^{13}\,\mathrm{cm}^{-5}$ from Table 7 to obtain

$$\mathcal{N}(\mathrm{N}) = 4.4 \times 10^5\,\mathrm{cm}^{-2} \text{ for } D = 88 \tag{12.11}$$

12.4 USE OF ESTIMATES OF EXPANSION VELOCITIES

In the absence of further information, we take the velocity distribution function $f(v)$ to be constant within some finite range, $v_1 \leqslant v \leqslant v_2$. Consistent with (12.4) this gives

$$f(v) = \frac{1}{(v_2 - v_1)} \text{ for } v_1 \leqslant v \leqslant v_2 \tag{12.12}$$

and the integral in (12.9) is

$$\int_{v_1}^{v_2} \left[\frac{f(v)}{v}\right]^2 dv = \frac{1}{v_1 v_2 (v_1 - v_2)}\,. \tag{12.13}$$

It then follows from (12.9) that

$$\mathcal{N}(\mathrm{N}) = \frac{1}{d}\left\{t^3 n(\mathrm{N}) \frac{N(\mathrm{N})}{N_e} v_2^3\right\}^{1/2} \epsilon\,, \tag{12.14}$$

where $\epsilon = [(1 - v_1/v_2)v_1/v_2]^{1/2}$. From Table 7 we have $D^3 n(\mathrm{N}) = 2.41 \times 10^{19}$ for $D = 88$. Using the ionization equilibria of Table 5 and the abundances of Table 9 we have $N(\mathrm{N})/N_e = 0.017$. We take $v_2 = v(\mathrm{max}) = 1370\,\mathrm{km\,s}^{-1}$ from Section 3.3. The quantity $\epsilon = [(1-x)x]^{1/2}$

with $x = v_1/v_2$ has a maximum value of $\epsilon = 0.5$ for $x = 0.5$ and is insensitive to x for $x \simeq 0.5$. If we adopt $v_1 = \bar{v} = 760\,\mathrm{km\,s^{-1}}$ from Section 3.3, we obtain $(v_1/v_2) = 0.55$ and $\epsilon = 0.50$. With $d = 2.2$ kpc we obtain

$$\mathcal{N}(\mathrm{N}) = 21 \times 10^5\,\mathrm{cm^{-2}} \text{ for } D = 88 \tag{12.15}$$

12.5 THE IONIZED MASS

Our two estimates of $\mathcal{N}(\mathrm{N})$ for $D = 88$, equations (12.11) and (12.15), differ by a factor of 4.5. We adopt the geometric mean, $\mathcal{N}(\mathrm{N}) = 10^6\,\mathrm{cm^{-2}}$, which is probably correct to within a factor of 2. From equation (12.9) and the observed approximate constancy of $D^3 n(\mathrm{N})$ we may conclude that $\mathcal{N}(\mathrm{N})$ is constant for $D \geqslant 70$. With $\mathcal{N}(\mathrm{N}) = 10^6\,\mathrm{cm^{-2}}$ and $d = 2.2$ kpc the total number of ionized nitrogen atoms is

$$4\pi d^2\,\mathcal{N}(\mathrm{N}) = 6 \times 10^{50}. \tag{12.16}$$

With the mass fractions of Table 9 the total ionized mass is

$$M_\mathrm{i} = 1.1 \times 10^{29}\,\mathrm{g} = 6 \times 10^{-5} M_\odot \text{ for } D \geqslant 70 \tag{12.17}$$

The ionized carbon mass is 4×10^{27} g which is much larger than the estimate of Gehrz *et al.* for the mass in grains, 5×10^{25} g.

The ionized mass, $6 \times 10^{-5} M_\odot$, is equal to the total ejected mass if the shell is fully ionized. This may be the case but there is some uncertainty, as discussed in Section 12.1.

12.6 THE KINETIC ENERGY

The kinetic energy is obtained on multiplying the mass by $\frac{1}{2}\langle v^2 \rangle$ where

$$\frac{1}{2}\langle v^2 \rangle = \int f(v) v^2\,dv. \tag{12.18}$$

Using (12.12), $\langle v^2 \rangle = (v_1^2 + v_1 v_2 + v_2^2)/3$ and with $v_1 = 760\,\mathrm{km\,s^{-1}}$, $v_2 = 1370\,\mathrm{km\,s^{-1}}$ we obtain

$$\frac{1}{2}\langle v^2 \rangle M_\mathrm{i} = 6 \times 10^{44}\,\mathrm{erg}. \tag{12.19}$$

13 The stellar remnant

13.1 TEMPERATURE OF THE REMNANT

The fluxes for typical nebular lines and for thermal infrared emission have maximum values on $D \simeq 60$. We can be confident that the nebula is optically thick for ionizing radiation for $D \leqslant 60$. We shall assume it to be optically thick for $D = 70$. More specifically, we assume the optical depth to be such that there is no escape of radiation with $\lambda \leqslant 912$ Å. The difference between the observed flux $F(\mathrm{obs})$ and the total flux $F(\mathrm{tot})$ is then due to Lyα and to radiation in the region $912 < \lambda < 1140$ Å. We have $F(\mathrm{obs}) = 3.89 \times 10^{-8}\,\mathrm{erg\,cm^{-2}\,s^{-1}}$. Using the results of Section 8.2 we calculate that the continuum radiation with $912 < \lambda < 1140$ Å is about 2 per cent of $F(\mathrm{obs})$. If we assume that 30 per cent of the Lyα flux is absorbed by dust we obtain $F(\mathrm{tot}) = 5.0 \times 10^{-8}\,\mathrm{erg\,cm^{-2}\,s^{-1}}$. In Section 8.3 we made the approximation of putting $F(\mathrm{tot}) = F(\mathrm{obs})$ and obtained $T_\mathrm{s} = 140\,000$ K for the star temperature. If the same method were used with the present estimate of $F(\mathrm{tot})$ we would obtain $T_\mathrm{s} = 150\,000$ K.

We may also attempt to estimate T_s using Zanstra methods. We cannot use, in any simple way, the He II Zanstra method, because it may be shown, with the abundances of Table 5, that the total rate of recombinations to ions with ionization potentials greater than that of He^+ will be larger than the number of recombinations to He^+ (for some of the ions dielectronic recombination gives large recombination rates). We therefore consider only the Zanstra H I method. We assume that each recombination of an ion other than H^+ gives one photon which ionizes H^0. The number of H^+ recombinations is then equal to the number of stellar quanta with $\lambda \leqslant 912$ Å:

$$\int_0^{\lambda_0} \frac{L_\lambda}{h\nu}\, d\lambda = \alpha_B(H^0) \int N_e N(H^+)\, dV, \tag{13.1}$$

where $\lambda_0 = 912$ Å. Dividing (13.1) by $4\pi d^2$

$$\int_0^{\lambda_0} \frac{F_\lambda}{h\nu}\, d\lambda = \alpha_B(H^0)\, n(H^+). \tag{13.2}$$

Let us suppose that the stellar continuum flux is observed at some wavelength λ_1 and that it has a blackbody distribution. We then obtain

$$\left(\frac{h\nu_1}{\lambda_1 F_{\lambda_1}}\right) \alpha_B(H^0)\, n(H^+) = G(T_s), \tag{13.3}$$

where

$$G(T_s) = \left(\frac{\exp(u_1) - 1}{u_1^3}\right) \int_{u_0}^{\infty} \frac{u^2}{\exp(u) - 1}\, du \tag{13.4}$$

and where $u_1 = (hc/\lambda_1 k T_s)$, $u_0 = (hc/\lambda_0 k T_s)$. We obtain $\alpha_B(H^0)\, n(H^+) = 720\ \mathrm{cm^{-2}\,s^{-1}}$, calculated as in Section 11.3. We take $\lambda_1 = 1400$ Å and $\lambda_1 F_{\lambda_1} = 1.6 \times 10^{-9}\ \mathrm{erg\,cm^{-2}\,s^{-1}}$. This gives

$$\left(\frac{h\nu_1}{\lambda_1 F_{\lambda_1}}\right) \alpha_B(H^0)\, n(H^+) = 6.4. \tag{13.5}$$

The function $G(T_s)$ is tabulated in Table 10. It is seen that the equation $G(T_s) = 6.4$ is satisfied for a value of T_s very close to our previous estimate, $T_s = 150\,000$ K.

13.2 LATER EVOLUTION OF THE REMNANT

We have seen that, for $D \geqslant 70$, $n(He^+)$ decreases approximately proportional to D^{-3}, and that the nebula remains optically thick for ionization of He^+. It follows that the number of

Table 10. The function $G(T_s)$ defined by (13.4), calculated for $\lambda_0 = 912$ Å, $\lambda_1 = 1400$ Å.

T_s	$G(T_s)$
50 000	0.620
100 000	2.79
150 000	6.18
200 000	10.73
250 000	16.42

stellar quanta which can ionize He^+ ($\lambda \leqslant 228$ Å) decreases like D^{-3}. For $D = 70$ we obtained, in Section 9, $R_s = 0.13 R_\odot$ for the radius of the remnant. If its temperature remains constant we obtain the required decrease in quanta with $\lambda < 228$ Å if R_s decreases like $D^{-3/2}$, giving $R_s = 0.014 R_\odot$ by $D = 304$. This seems improbable, since the radius of a white dwarf is about $0.015\ R_\odot$. We conclude that there must be a decrease in T_s as well as in R_s.

14 Summary and discussion

14.1 SUMMARY

Our main conclusions from interpretation of observations of Nova Cygni 1978 are:

(a) The reddening is $E(B-V) = 0.4 \pm 0.1$ from the λ 2200 feature.

(b) A distance of $d = 2.2$ kpc is obtained on equating the maximum luminosity to the Eddington luminosity. This is in good agreement with the distance deduced by Duerbeck *et al.* from a relation between reddening and distance but is smaller than the distance deduced from the relation between decay time and maximum absolute visual magnitude.

(c) The number of CNO atoms in the shell, relative to H, is larger than the number in the Sun by a factor of 30. There is a particularly large enhancement for N, by a factor of 200.

(d) The mass of ionized gas in the ejected shell is 1.1×10^{29} g and its kinetic energy is 6×10^{44} erg. There is some evidence that the ionized mass is equal to the total ejected mass but this evidence is not conclusive.

(e) The total luminosity of the remnant has an approximately constant value of $L = 1.7 \times 10^4 L_\odot$ from $D = 13$–27 (D is the number of days after outburst).

(f) For $D = 70$ the stellar remnant had a temperature of $T_s = 1.5 \times 10^5$ K, a radius of $R_s = 0.13 R_\odot$ and a luminosity of $L = 8 \times 10^3 L_\odot$.

(g) For $D > 70$, the numbers of quanta with $\lambda < 228$ Å decrease proportional to D^{-3}. This is probably due to decreases in both T_s and R_s.

(h) There is a high efficiency (about 80 per cent) for conversion of He II Lyα to quanta in O III Bowen lines.

(i) The onset of thermal infrared emission is due to the heating of pre-existing dust by absorption of radiation in UV resonance lines.

14.2 DISCUSSION

As noted in Section 1, our work indicates that Nova Cygni 1978 was produced by a thermonuclear runaway in material accreted on to a white dwarf. The main evidence comes from our determination of the chemical composition of the ejected material, which we believe to be more accurate than previous determinations of abundances in nova ejecta. Our results indicate that, prior to the runaway, the material in the envelope had C and O abundances enhanced by a factor of about 20, compared with solar abundances. An enhancement by this amount is sufficient to ensure that the energy generated in the runaway would be large enough to eject a shell. The nuclear reactions which occur during the runaway produce a large amount of nitrogen. The very large enhancement which we obtain for the nitrogen abundance in the ejected material, by a factor of about 200 compared with the Sun, is fully in accord with predictions for material processed by a thermonuclear runaway.

We may attempt a comparison with the models of Starrfield *et al.* (1978). The closest agreement is with their model 1, for which it is assumed that an envelope of $1.26 \times 10^{-3} M_\odot$ is accreted onto a white dwarf of mass $1.0 M_\odot$. The initial composition of the envelope material is taken to be $X(C) = X(O) = 0.04$. Table 11 gives, for model 1 and for Nova

Table 11. Comparison of Nova Cygni 1978 with model 1 of Starrfield *et al.* (1978).

	M_V (max)	M_{ej} (10^{29} g)	Shell KE (10^{44} erg)	Shell mass fractions X(C)	X(N)	X(O)
Model 1	−7.52	2	8.5	0.013	0.076	0.024
Nova Cyg 1978	− 6.71	1.1	6	0.04	0.14	0.13

Cygni 1978: maximum absolute visual magnitude, M_V (max); the ejected mass M_{ej} (for Nova Cygni we take this to be equal to the ionized mass); the shell kinetic energy, KE; and mass fractions X(C), X(N) and X(O) for the ejected material. There is seen to be reasonable agreement for M_V (max), M_{ej} and KE (we recall that Nova Cygni 1978 appears to be underluminous in M_V (max)). The total CNO abundances assumed for the model are lower than those deduced for Nova Cygni 1978. For the model, all of the nitrogen in the ejected material is produced by the nuclear reactions and the total amount of nitrogen ejected, $M_{ej}X$(N), provides a measure of the amount of energy produced by the nuclear reactions. This amount is $M_{ej}X(\mathrm{N}) = 1.5 \times 10^{28}$ g for model 1 and 1.3×10^{28} g for Nova Cygni. Since the values of KE are nearly the same, the close agreement in the values of $M_{ej}X$(N) is very satisfactory.

The large total luminosity which we obtain for some time after outburst is consistent with predictions from the models, that hydrogen burning continues to occur in accreted material which is not ejected. Our estimate for the radius of the remnant on $D = 70$, $R_s = 0.13R_\odot$, may be compared with the radius of a white dwarf, R(WD) $\simeq 0.015R_\odot$.

Acknowledgments

In the present paper we have made extensive use of data which other observers have provided in advance of publication; to all concerned we express our sincere thanks. We also thank Drs H. W. Duerbeck and J. P. Harrington for very helpful comments on an earlier version of the present paper.

References

Baluja, K. L., Kingston, A. E. & Burke, P. G., 1980. *J. Phys. B: Atom. Molec. Phys.*, **13**, 829.
Bates, D. R. & Massey, H. S. W., 1943. *Phil. Trans. R. Soc.*, **A239**, 269.
Bode, M. F. & Evans, A., 1980. *Astr. Astrophys.*, **89**, 158.
Brocklehurst, M., 1971. *Mon. Not. R. astr. Soc.*, **153**, 471.
Canterna, R. & Schwartz, R. D., 1977. *Astrophys. J.*, **216**, L91.
Cassatella, A., Benvenuti, P., Clavel, J., Heck, A., Penston, M., Selvelli, P. L. & Macchetto, F., 1979. *Astr. Astrophys.*, **74**, L18.
Clavel, J., Flower, D. R. & Seaton, M. J., 1981. *Mon. Not. R. astr. Soc.*, **197**, 301.
Crampton, D., 1979. *Astrophys. J.*, **230**, 717.
Duerbeck, H. W., Rindermann, K. & Seitter, W. C., 1980. *Astr. Astrophys.*, **81**, 157.
Dufton, P. L., Berrington, K. A., Burke, P. G. & Kingston, A. E., 1978. *Astr. Astrophys.*, **62**, 111.
Fehrenbach, C. & Andrillat, C. R., 1979. *C. r. Acad. Sci. (Paris)*, **288B**, 191.
Ferland, G. J. & Shields, G. A., 1978. *Astrophys. J.*, **226**, 172.
Gallagher, J. S. & Code, A. D., 1974. *Astrophys. J.*, **189**, 303.
Gallagher, J. S. & Starrfield, S., 1978. *A. Rev. Astr. Astrophys.*, **16**, 171.
Gallagher, J. S., Kaler, J. B., Olson, E. C., Hartkopf, W. I. & Hunter, D. A., 1980. *Publs astr. Soc. Pacif.*, **92**, 46.
Gehrz, R. D., Hackwell, J. A., Grasdalen, G. L., Ney, E. P., Negebauer, G. & Sellgren, K., 1980. *Astrophys. J.*, **237**, 855.

Harrington, J. P., 1972. *Astrophys. J.*, **176**, 127.
Harrington, J. P., Lutz, J. H., Seaton, M. J. & Stickland, D. J., 1980. *Mon. Not. R. astr. Soc.*, **191**, 13.
Harrington, J. P., Lutz, J. H. & Seaton, M. J., 1979. *The First Year of IUE*, p. 199, ed. Willis, A. J., University College London.
Hummer, D. G. & Kunasz, P. B., 1980. *Astrophys. J.*, **236**, 609.
Jackson, A. R. C., 1973. *Mon. Not. R. astr. Soc.*, **165**, 53.
Joseph, R. D., Kessler, M. F. & Selby, M. J., 1981. *Mon. Not. R. astr. Soc.*, to be submitted.
Klare, G., Wolf, B. & Krautter, J., 1980. *Astr. Astrophys.*, **89**, 282.
Lambert, D. L., 1978. *Mon. Not. R. astr. Soc.*, **182**, 249.
McLaughlin, D. G., 1960. *Stellar Atmospheres*, p. 585, ed. Greenstein, J., Chicago University Press.
Mustel, E. R. & Boyarchuk, M. E., 1959. *Sov. Astr. – A. J.*, **3**, 744.
Pottasch, S., 1959. *Ann. Astrophys.*, **22**, 412.
Pradhan, A. K., 1976. *J. Phys. B: Atom. Molec. Phys.*, **9**, 433.
Saraph, H. E. & Seaton, M. J., 1980. *Mon. Not. R. astr. Soc.*, **193**, 617.
Schmidt, T., 1957. *Z. Astrophys.*, **41**, 182.
Seaton, M. J., 1975. *Mon. Not. R. astr. Soc.*, **170**, 474.
Seaton, M. J., 1978. *Mon. Not. R. astr. Soc.*, **185**, 5P.
Seaton, M. J., 1979. *Mon. Not. R. astr. Soc.*, **187**, 73P.
Seaton, M. J. & Storey, P. J., 1976. *Atomic Processes and Applications*, p. 131, ed. Burke, P. G. & Moiseiwitsch, B. L., North-Holland, Amsterdam.
Slovak, M. H. & Vogt, S. S., 1979. *Nature*, **277**, 114.
Starrfield, S., Truran, J. W. & Sparks, W. M., 1978. *Astrophys. J.*, **226**, 186.
Stickland, D., Penn, C. J., Seaton, M. J., Snijders, M. A. J., Storey, P. J. & Kitchin, C. R., 1979. *The First Year of IUE*, p. 63, ed. Willis, A. J., University College London.
Storey, P. J., 1981. *Mon. Not. R. astr. Soc.*, **195**, 27P.
Taylor, P. O., Gregory, D., Dunn, G. H., Phaneuf, R. A. & Crandall, D. H., 1977. *Phys. Rev. Lett.*, **39**, 1256.
Weymann. R. J. & Williams, R. E., 1969. *Astrophys. J.*, **157**, 1201.
Williams, R. E., Woolf, N. J., Hege, E. K., Moore, R. L. & Kopriva, D. A., 1978. *Astrophys. J.*, **224**, 171.
Wu, C. C., Boggess, A., Holm, A. V., Penny, P. M., Schiffer, F., Tunrose, B. E. & West, D. K., 1979. *Bull. Am. astr. Soc.*, **10**, 687.
Wyngaarden, W. L. & Henry, R. J., 1976. *J. Phys. B: Atom. Molec. Phys.*, **9**, 1461.